Ab Initio Quantum Chemical Study of the Coordination Preferences and Catalytic Role of Cu⁺ Ions in the Dehydration Reactions of Hydroxyformaldoxime Conformers and the Oxidation of HCN to Hydroxyformaldoxime by Hydrogen Peroxide

Dimitrios A. Pantazis, Athanassios C. Tsipis, and Constantinos A. Tsipis*

Laboratory of Applied Quantum Chemistry, Faculty of Chemistry, Aristotle University of Thessaloniki, 540 06 Thessaloniki, Greece

A detailed exploration of the configurational and conformational space of hydroxyformaldoxime (hfaox) has been carried out with the aid of first principles quantum chemical techniques at the HF, MP2, B3LYP, and CCSD(T) levels of theory using the 6-31G(d), 6-311G(d,p), 6-311+G(2df,2p), and 6-311++G(2d,p) basis sets. The most stable configuration among the eight possible hfaox conformers corresponds to the (*Z*)-(*s*-cis,*s*-trans) configuration, while the highest energy (*E*)-(*s*-trans,*s*-cis) conformer was found at 15.26, 15.31, 14.34, 14.91, and 14.78 kcal/mol higher in energy at the HF, MP2, B3LYP, MP4SDQ, and CCSD(T) levels of theory, respectively, using the largest 6-311++G(2d,p) basis set. Calculated structures, relative stability, and bonding properties of the conformers are discussed with respect to computed electronic and spectroscopic properties, such as charge density distribution, harmonic vibrational frequencies, and NMR chemical shifts. From a methodological point of view, our results confirm the reliability of the integrated computational tool formed by the B3LYP density functional model. This model has subsequently been used to investigate the dehydration reactions of hfaox. Upon dehydration, hfaox could afford a number of isomeric CHNO species. All dehydration processes, except those yielding cyanic acid, are predicted to be endothermic. The most endothermic one is the dehydration reaction of the more stable (*Z*)-(*s*-cis,*s*-trans) conformer, **7**, to formylnitrene, with the computed heat of reaction ($\Delta_R H$) being equal to 51.34 kcal/mol. On the other hand, the most exothermic dehydration process is the dehydration reaction of the (*E*)-(*s*-trans,*s*-cis) conformer, **14**, to cyanic acid with the computed heat of reaction being equal to −26.16 kcal/mol at the B3LYP/6-311G(d,p) level of theory. The reaction pathway for the addition of water to fulminic acid is predicted to occur via an activation barrier of 68.18 kcal/mol at the B3LYP/6-311G(d,p) level. The interaction of Cu⁺ ions with the CHNO isomers, as well as their precursor hfaox conformers, was also analyzed in the framework of DFT theory, illustrating that the Cu⁺ ions show a higher affinity for the N donor atoms. Depending on the conformer, the computed interaction energies for the Cu−N, Cu−ON, and Cu−OC associations in the Cu(hfaox)⁺ complexes were found in the range of 62.61−75.29, 44.75−57.43, and 38.84−58.46 kcal/mol, respectively. In summary, the calculations threw light on the bonding properties of the CHNO species, being the simplest model of the HN−CO peptide linkage to biologically important Cu⁺ ions. Of particular interest is the prediction that Cu⁺ ions catalyze the dehydration reactions of hfaox to form CHNO isomers and are involved in a novel reaction of the oxidation of organic nitriles with hydrogen peroxide to yield oximes, the latter process providing a novel synthetic route for oxime derivatives. The energetic and geometric profiles of these reactions were fully investigated in the framework of DFT theory, and their mechanisms are thoroughly discussed.

Introduction

The isomeric CHNO molecules and their substituted derivatives C(X)NO (X = F, Cl, OH, NH₂, CN, alkyl and aryl groups) are an important class of compounds that have a large variety of applications in organic, bioorganic, and polymer chemistry.[1] The decomposition reactions of the CHNO isomers play an important role in the combustion of N-containing hydrocarbon fuels.[2] Moreover, these reactions are characteristic reactions of the practically important rapid reduction of nitrogen oxides (RAPRENO) process, which involves removal of NO$_x$ combustion products by the injection of cyanuric acid, (HOCN)₃, into the exhaust stream.[3] Detailed investigation of the CHNO potential energy surface[4−10] suggested that the more stable

CHNO isomers are the isocyanic (**1**), cyanic (**2**), fulminic (formonitrile oxide, **3**), and isofulminic (carboxime, **4**) acids (Scheme 1). Isocyanic and fulminic acids have been experimentally well-characterized molecules; the other two isomers are likely to be reasonably stable species and should be observable under suitable conditions.[11] Other conceivable CHNO isomers such as formylnitrene (**5**), and oxazirine (**6**) were found to collapse with little or no activation to more stable isomers.

Global potential energy surfaces (PES) of the [H,C,N,O] system in singlet and triplet states have thoroughly been investigated by Mebel et al.[9] at the B3LYP/6-311G(d,p) level of theory. The global features of the singlet and triplet PES have been applied to several important fragmentation and decomposition reactions, their major product channels have been speculated, and the activation energies have been reported.

* To whom correspondence should be addressed. Tel.: (+031) 997851. Fax: (+031) 997851. E-mail: tsipis@chem.auth.gr.

SCHEME 1: Possible Dehydration Products of Hydrohyformaldoxime
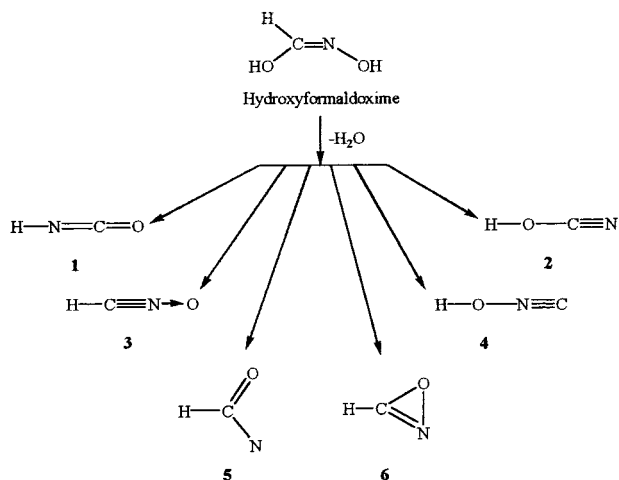
Moreover, an exhaustive ab initio quantum chemical study of the PES governing the isomerization and dissociation reactions of the CHNO isomers has recently been reported by Shapley and Bacskay.[10] It was found that the lowest energy pathways for the isomerization of the open-chain species are two-step reactions that proceed via cyclic intermediates.

Some of the CHNO molecules react not only with unsaturated substrates to afford 1,3-dipolar cycloaddition products but also with nucleophilic reagents, including both anionic and neutral nucleophiles, providing thus open-chain oximes as products. The ease of deformation of formonitrile oxide, the formation of hydrogen-bonded complexes with water, and the reaction pathway with water as nucleophile (HCNO + $H_2O \rightarrow$ HOCH=NOH) have been studied earlier[12] at the HF/STO-3G level of theory and reinvestigated later[13] at higher levels of theory (HF/3-21G, HF/6-31G*, MP2/6-31G*, MP4−SDQ/6-31G*, and MP2/6-31G**) to determine whether the mechanism of neutral nucleophilic addition to nitrile oxide is concerted or stepwise. In the present paper, we thought that it would be advisable to further investigate through first principles quantum chemical techniques of high quality the configurational, conformational, energetic, electronic, and spectroscopic properties of hydroxyformaldoxime (hfaox), HOCH=NOH, and its possible dehydration CHNO products (Scheme 1). In addition, we report on the details of the exploration of the coordination ability of hfaox and its dehydration products toward Cu^+ ions, pursuing a threefold objective: (i) the examination of the preferred coordination sites of the hfaox conformers and their dehydration CHNO isomeric products to Cu^+ ions; (ii) the exploration of the role played by the Cu^+ ions in the dehydration reactions of hfaox conformers; (iii) the understanding of the bonding properties of the HNCO species, being the simplest model of the HN−CO peptide linkage to biologically important Cu^+ ions. The structural, energetic, electronic, and spectroscopic (IR, NMR) properties were computed by a variety of theoretical methods (HF, MP2, MP4SDQ, CCSD(T), and B3LYP) using 6-31G(d), 6-311G(d,p), 6-311+G(2df,2p), and 6-311++G(2d,p) basis sets wishing to identify levels of theory suitable for general application. The effect of level of theory on the structural, energetic, electronic, and spectroscopic properties of the compounds was also examined, and the results are discussed in relation with available experimental and theoretical data.

Computational Details

Standard ab initio molecular orbital theory[14] and density functional theory (DFT)[15] were carried out using the Gaussian 98 program suite.[16] The geometries of the hydroxyformaldoxime (hfaox), HOCH=NOH, conformers were fully optimized at the HF, MP2, CCSD(T), and Becke's three-parameter hybrid functional combined with the Lee−Yang−Parr correlation functional, abbreviated as B3LYP, level of density functional theory using 6-31G(d), 6-311G(d,p), 6-311+G(2df,2p), and 6-311++G(2d,p) basis sets. Moreover, single-point energy calculations used the MP4SDQ and CCSD(T) methods combined with the largest basis set. The geometries of the CHNO isomers and their complexes with Cu^+ ions were fully optimized at the B3LYP level of theory using the 6-311G(d,p) basis set. In all computations, no constrains were imposed on the geometry. Full geometry optimization was performed for each structure using Schlegel's analytical gradient method,[17] and the attainment of the energy minimum was verified by calculating the vibrational frequencies that result in absence of imaginary eigenvalues. All of the stationary points have been identified for minimum (number of imaginary frequencies (NIMAG) = 0) or transition states (NIMAG = 1). The vibrational modes and the corresponding frequencies are based on a harmonic force field. This was achieved with the SCF convergence on the density matrix of at least 10^{-9} and the rms force less than 10^{-4} au. All bond lengths and bond angles were optimized to better than 0.001 Å and 0.1°, respectively. The computed electronic energies, the enthalpies of the dehydration reactions ($\Delta_R H$), and the activation energies ($\Delta G^{\ddagger}$), were corrected to constant pressure and 298 K for zero-point energy (ZPE) differences and for the contributions of the translational, rotational, and vibrational partition functions. For transition states geometry determination, QST2 and QST3 computations were performed, giving identical results for each reaction separately. Moreover, corrections of the transition states have been confirmed by intrinsic reaction coordinate (IRC) calculations, while intrinsic reaction paths (IRPs)[18] were traced from the various transition structures to make sure that no further intermediates exist. Magnetic shielding tensors have been computed with the GIAO (gauge-including atomic orbitals) DFT method[19] as implemented in the Gaussian 98 series of programs[16] employing the B3LYP level of theory.

Results and Discussion

Configurations and Conformations of Hydroxyformaldoxime. Hydroxyformaldoxime (hfaox), HOCH=NOH, can exist in either *Z* or *E* configurations with respect to the C=N double bond and in the conformations *s*-cis and *s*-trans with respect to the C−O and N−O single bonds. The eight possible conformers of hfaox, along with their structural parameters, relative stability, and dipole moments computed at the B3LYP/6-311G(d,p) level of theory, are shown in Figure 1. All structures corresponding to local minima in the PES exhibit planar geometry. The optimized structures (under the constrains of keeping the CH and OH bond lengths constant) and relative energies of hydroxyformaldoxime isomers have been computed two decades ago at the minimal-basis HF/STO-3G level of theory as part of a theoretical study of the reaction of water with the 1,3 dipoles fulminic acid and acetonitrile oxide.[12]

Calculated Structures and Stability. The computed equilibrium structures of all (eight) possible conformers of hfaox at the selected levels of theory are summarized in the Supporting Information (Tables S1 and S2). The HF method underestimates the bond lengths by up to 0.045 Å with respect to the correlated MP2, B3LYP, and CCSD(T) methods, the latter being used to produce benchmark results. The B3LYP approach gives almost identical bond lengths (bond lengths differ less than 0.009 Å)
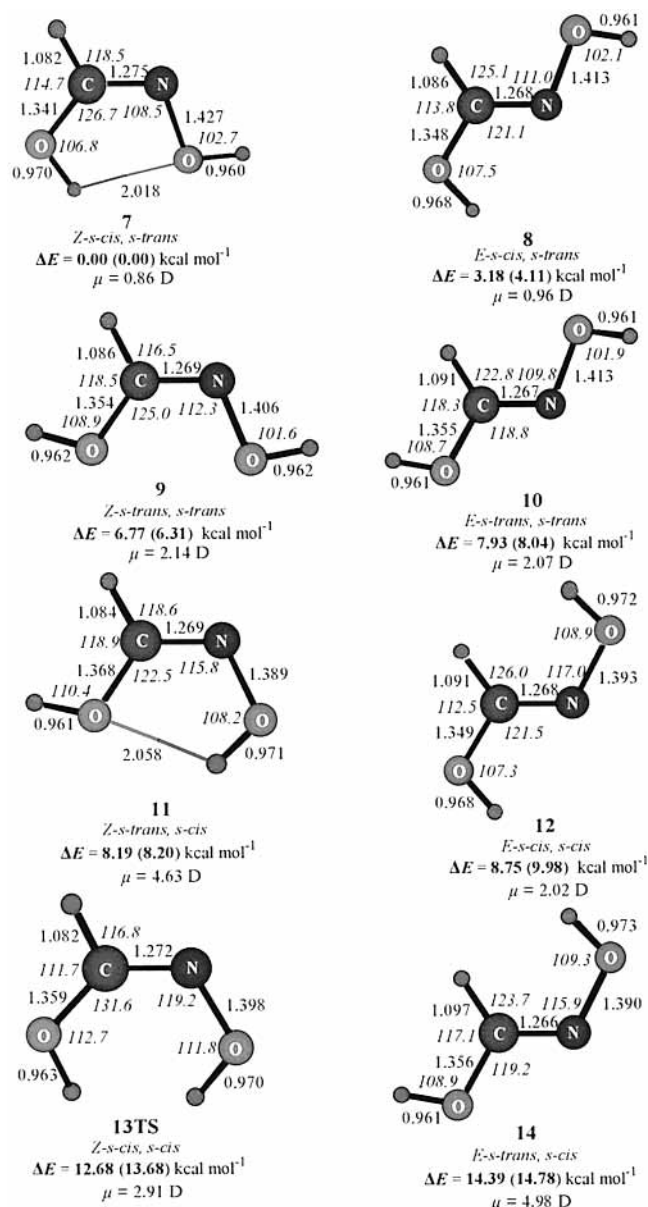
Ab Initio Quantum Chemical Study

J. Phys. Chem. A, Vol. 106, No. 7, 2002 **1427**

Figure 1. Equilibrium structures (bond lengths in Å, bond angles in deg), relative stability (in kcal/mol) and dipole moments of hfaox conformers, computed at the B3LYP/6-311G(d,p) level of theory. Figures in parentheses are the relative energies computed at the CCSD(T)/6-311++G(2d,p)//B3LYP/6-311G(d,p) level of theory.

to those of the CCSD(T) method. The same is also true for the correlated MP2 approach which produces bond lengths in close agreement with those of the highest level CCSD(T) method for each basis set used. In all conformers, because of resonance, the NO single bond is shorter than a NO single bond (r(N−O) = 1.44 Å) and the CN bond is longer than a CN double bond (r(C=N) = 1.265 Å). In general terms, bond angles are little sensitive to the level of calculation and enlargement of basis set from 6-31G(d) to 6-311++G(2d,p). There is only an overestimation of the ∠ONC, ∠HOC, and ∠HON bond angles by up to 2°−3° at the uncorrelated HF method as compared to MP2, B3LYP, and CCSD(T) methods. Interestingly, the quality of basis set has also no significant effect on the structural parameters of the hfaox conformers. The good performance of computationally less-expensive methods, particularly B3LYP and MP2 in conjunction with basis sets incorporating at least polarization functions, offers a reliable alternative for geometry

predictions of hfaox conformers. Therefore, we decided to choose the computationally less-expensive B3LYP/6-311G(d,p) procedure for the investigation of the structural and spectroscopic properties of the hfaox conformers, the dehydration products, and their associations with Cu⁺ ions.

In general terms, relative stability of hfaox conformers is little sensitive to the level of calculation, and enlargement of the basis set never changes B3LYP relative energies by more than 1.0 kcal/mol (Table S3, Supporting Information). Our best estimate of the relative stability of hfaox conformers is obtained at the more sophisticated CCSD(T)/6-311++G(2d,p)//B3LYP/6-311G(d,p) level of theory and these results are again used as benchmark results (Figure 1). It can be seen that the chosen computationally less-expensive B3LYP/6-311G(d,p) model for all calculations predicts relative stabilities of conformers very close to those of the more sophisticated CCSD(T)/6-311++G(2d,p)// B3LYP/6-311G(d,p) one, the changes observed being less than 1.2 kcal/mol.

The highest energy conformer corresponding to the (*E*)-(*s*-trans,*s*-cis) isomer, **14**, was found at 14.39 kcal/mol higher in energy than the more stable (*Z*)-(*s*-cis,*s*-trans) isomer, **7**. The (*Z*)-(*s*-cis,*s*-cis) isomer, **13TS**, possesses one imaginary frequency and therefore is the transition state for a possible *s*-trans,*s*-cis → *s*-cis,*s*-trans isomerization process of the conformers with a Z-configuration, namely, the **11** → **7** isomerization with an activation barrier of 4.95 kcal/mol at the B3LYP/6-311G(d,p) level of theory. The high stability of **7** could be attributed to hydrogen bond formation between the H atom of the C−OH group and the O atom of the N−OH group. All conformers with Z-configuration are slightly more stable than those having the E-configuration. Considering that the electronic factors of the hfaox isomers are similar, their relative stability could be accounted for by steric factors. The interconversion processes of the conformers involve rotation around the N−O or C−O single bonds, the computed rotation barrier being equal to 4.0−7.0 kcal/mol. These results are in line with other reported studies on *s*-cis,*s*-trans isomerization.[12,20]

Electronic Properties and Bonding. The sequence of Kohn−Sham molecular orbitals (MOs) deduced for the conformers **7**, **9**, **11**, **12**, and **14** is ...(11a′)²(1a″)²(12a′)²(2a″)²(13a′)²(3a″)². For conformers **8**, **10**, and **13TS**, there is an inversion of the 11a′ and 1a″ and 12a′ and 2a″ MOs and the sequence is ...(1a″)²(11a′)²(2a″)²(12a′)²(13a′)²(3a″)². The 3a″ HOMO (highest occupied molecular orbital) of all hfaox conformers corresponds to a C=N bonding in conjunction with C−O and N−O antibonding combination of π-type orbitals spanning all heavy atoms. The LUMO (lowest unoccupied molecular orbital) exhibiting a′ symmetry (14a′ MO) corresponds to a nonbonding MO localized either on the H atom of the H−O−C moiety (conformers **9**, **10**, **11**, **13TS**, and **14**) or the H atom of the H−O−N moiety (conformer **12**) or on both (conformers **7** and **8**). The respective π*-MO exhibiting also a′ symmetry corresponds either to LUMO+1 (conformers **7**, **11**, and **13TS**) or LUMO+2 (conformers **8**, **9**, **10**, **12**, and **14**). The HOMO−LUMO energy gap being equal to 6.35−7.34 eV follows the trend **7** > **8** > **12** > **9** > **14** > **10** > **11** > **13TS**.

According to the Mulliken population analysis given in the Supporting Information (Figure S1), there are no significant changes on both net atomic charges and bond overlap populations (bop) in hfaox conformers. In conformers **7**−**10**, the hydrogen atoms of the NO−H moiety acquire a little more positive net atomic charge with respect to those of the CO−H moiety. However, the opposite is true for conformers **11**, **12**, **13TS**, and **14**. The positively charged NO−H and CO−H

hydrogen atoms combined with the nature of the LUMO comprise the electrophilic centers of the conformers. On the other hand, both oxygen atoms are more negatively charged relative to the nitrogen atom and in conjunction with the nature of the HOMO are the nucleophilic centers of the conformers. Moreover, the C−O bond is much stronger than the N−O one.

Infrared Spectra. We only analyze the infrared spectra of the more stable conformer, **7**, as most of the computed harmonic vibrational frequencies and the corresponding normal modes are not sensitive to configurational and conformational changes. The computed harmonic vibrational frequencies and the corresponding normal modes for all hfaox conformers at both the MP2/6-31G(d) and B3LYP/6-31G(d) levels of theory are listed in detail in the Supporting Information (Tables S4, S5). The two high-frequency normal modes in the region of 3600−3800 cm^{-1} could be assigned to ν(O−H) stretching vibrations of the N−OH and C−OH moieties, the former absorbing at higher frequencies. The next strong band in the region of 1706−1781 cm^{-1} originates from the ν(C=N) stretching vibration. Values for this fundamental in the CH$_3$(H)CNOH,[21] (CH$_3$)$_2$CNOH,[22] and X$_2$CNOH[20] (X = Cl, Br) oximes are 1655, 1675, 1603, and 1597 cm^{-1}, respectively. Obviously, the computed harmonic ν(C=N) stretching frequency is in surprisingly good agreement with the above values, considering the well-known overestimation of the harmonic vibrational frequencies by the ab initio computational techniques. The frequency scaling factor suitable for fundamental vibrations at the MP2/6-31G(d) and B3LYP/6-31G(d) level was evaluated[23] to be 0.9427 and 0.9614, respectively. In the region of 1111−1501 cm^{-1}, the relatively strong IR bands ascribable to ν(C−H) stretching strongly coupled with NOH and COH bending vibrations are predicted to occur. The ν(N−O) stretching vibrational frequency appearing in the region of 920−1007 cm^{-1} is shifted by about 30−70 cm^{-1} to higher wavenumbers in *E*-conformers with respect to *Z*-conformers. Therefore, the ν(N−O) band can be used as a good criterion for distinguishing the *Z*- and *E*-conformers of hfaox. It should be noted that the NO stretch in oximes typically appears around 930 cm^{-1}. The band in the region of 380.0−622.0 cm^{-1} showing a C-type envelope is assigned to COH torsion strongly coupled with CNOH out-of-plane deformation, while the weak band at very low frequencies, namely, at 114−288 cm^{-1}, is ascribed to strongly coupled NOH and COH torsional vibrations. Both of these bands, being sensitive to configurational and conformational changes, could be used as a guide for distinguishing experimentally by IR spectra *Z/E*-configurations and *s*-cis,*s*-trans conformations of hfaox.

NMR Spectra. By employing gradient-corrected levels of DFT, ^{13}C, ^{15}N, ^{17}O, and ^{1}H chemical shifts were calculated at the GIAO/B3LYP/6-311+G(2df,2p) level of theory using the B3LYP/6-311G(d,p) optimized geometries. The calculated absolute isotropic shielding tensor elements (σ, ppm) for hfaox conformers are summarized in the Supporting Information (Table S6). The absolute isotropic shielding tensor elements for the CH$_4$, NH$_3$, and H$_2$O molecules used as external reference standards for the gas-phase NMR are also given in Table S6. Notice that the computed NMR spectra of hfaox conformers are predictions because there are no experimental data available so far. The calculated chemical shift (δ, ppm) equals the difference between the shielding of the reference and the shielding of the molecule of interest, $\delta = \sigma_{\text{ref}} - \sigma$. Therefore, it is easy to convert absolute to relative chemical shifts. The conformational averaged GIAO/B3LYP ^{13}C, ^{15}N, ^{17}O, and^{1}H chemical shifts are summarized in Table 1.

TABLE 1: The Conformational Averaged GIAO/B3LYP/6-311+G(2df,2p)//B3LYP/6-311G(d,p) ^{13}C, ^{15}N, ^{17}O, and ^{1}H Chemical Shifts for Hydroxyformaldoxime Conformers

nucleus	δ (ppm)^a
^{13}C	157.9
^{15}N	341.5
^{17}O (N−OH)	169.3
^{17}O (C−OH)	114.8
^{1}H (C−H)	7.4
^{1}H (N−OH)	5.1
^{1}H (C−OH)	5.0

^{a} The external reference standards used for the ^{13}C, ^{14}N, ^{17}O, and ^{1}H NMR spectra were the CH$_4$, NH$_3$, H$_2$O, and TMS molecules, respectively.

The computed ^{13}C chemical shifts of the hfaox conformers found in the range of 150.7−164.5 ppm are characteristic of a nearly sp^2-hybridized carbon atom (compare with the experimental values of 130.6, 136.3, 137.9, 152.9, and 156.7 ppm for the ethene, formaldehyde, benzene, 2-hydroxyaryl ketoxime, and monoprotonated guanidine molecules, respectively, as well as to many other oxime molecules).[24−26] There is a small deshielding effect (2.9−10.3 ppm) going from *Z*- to *E*-configurations.

The ^{15}N chemical shifts found in the range of 330.9−361.0 ppm show a good agreement with the experimental values for oxime molecules.[27] Notice also that the experimental values[28,29] of ^{15}N chemical shift for N*N*O, 5-methylisoxazole and 3,5-dimethylisoxazole are 253.2, 254.6, and 263.9 ppm, respectively. The ^{15}N chemical shifts are more sensitive to configurational and conformational changes. There is a stronger deshielding effect (4.5−23.1 ppm) going from *Z*- to *E*-configurations.

The ^{17}O(N*O*H) chemical shifts of the hfaox conformers found in the range of 159.6−184.9 ppm are very close to the experimental value[24] of 143.4 ppm for the NNO molecule. For the couple of conformers **9**−**10** and **11**−**14**, a shielding effect amounting to 16.0 and 7.2 ppm, respectively, is observed, while for the couple of conformers **7**−**8** and **12**−**13TS**, a deshielding effect amounting to 5.1 and 0.3 ppm, respectively, is observed.

The ^{17}O(C*O*H) chemical shifts of the hfaox conformers are found in the range of 104.1−131.0 ppm. They all show an opposite behavior to that of ^{13}C chemical shifts exhibiting a shielding effect going from *Z*- to *E*-configurations, being more pronounced for the **7**−**8** and **9**−**10** couples (20.9 and 14.4 ppm, respectively). Unfortunately, no experimental data are available so far for comparisons to be made.

The ^{1}H(C*O*H) and ^{1}H(N*O*H) chemical shifts are found in the range of 3.3−8.6 ppm. In general terms, in conformers **7**, **11**, and **14**, the ^{1}H(C*O*H) chemical shifts are higher than ^{1}H(N*O*H) chemical shifts, while the opposite is true for conformers **8**−**10**. In conformers **12** and **13TS**, ^{1}H(C*O*H) and ^{1}H(N*O*H) chemical shifts are nearly the same. Surprisingly, the ^{1}H(N*O*H) chemical shifts are almost insensitive to configurational and conformational changes. The computed ^{1}H(C*O*H) and ^{1}H(N*O*H) chemical shielding tensor elements (absolute chemical shifts, σ, ppm) given in Table S6 (Supporting Information) compare well with those of CH$_4$, NH$_3$, and H$_2$O molecules at the B3LYP/6-311+G(2df,2p)//B3LYP/6-311G(d,p) level, being 31.5, 31.8, and 31.3 ppm, respectively. Notice that the experimental values of the ^{1}H NMR chemical shifts of CH$_4$, NH$_3$, and H$_2$O molecules are 30.93 ± 0.33, 30.68 ± 0.6, and 30.03 ± 0.6, respectively.

Finally, the ^{1}H(*H*CO) chemical shifts found in the range of 6.7−8.5 ppm are characteristic of ^{1}H NMR chemical shifts of hydrogen atoms bound to nearly sp^2-hybridized carbon atoms. They all show a parallel behavior to that of ^{13}C chemical shifts exhibiting a shielding effect going from *Z*- to *E*-configurations.

Ab Initio Quantum Chemical Study

J. Phys. Chem. A, Vol. 106, No. 7, 2002 **1429**

Dehydration Products of Hydroxyformaldoxime Conformers. Hydroxyformaldoxime is expected to exist in aqueous solutions of formonitrile oxide, as a result of the reaction with water nucleophile according to the chemical equation

$$HCNO + H_2O \rightarrow HOCH=NOH$$
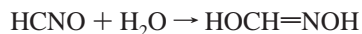
Among the 38 possible, topologically different, bound CHNO isomers we focus our attention on the six potentially stable species, given in Scheme 1, that are possible dehydration products of hfaox. The dehydration reaction of the more stable conformer **7** could afford directly, via an intramolecular water elimination reaction, either **5** (or its cyclic oxazirine isomer, **6**) or **4**. Conformer **11** is dehydrated either to **3** or **4**. Isofulminic acid could also be the dehydration product of conformers **9**, **10**, and **14**, while cyanic acid could result from dehydration of conformers **8**, **12**, and **14**. Finally, isocyanic acid could not be a direct dehydration product of hfaox conformers. Obviously, aqueous solutions of all isomers, except isocyanic acid, might be expected to contain significant amounts of hfaox conformers.

Calculated Structures, Relative Stabilities, and Bonding. The equilibrium structures and relative stability of the CHNO isomers in both their singlet and triplet states have thoroughly been investigated by Mebel et al.[9] at the same level of theory. Overall, our results are identical to those reported by Mebel et al.,[9] and therefore, only the more significant points of the structures of CHNO species related to their association with Cu^+ ions and the dehydration of hfaox conformers will be stressed herein. The equilibrium structures of the six CHNO isomers along with the net atomic charges, bond overlap populations, relative stability, and dipole moments computed at the B3LYP/6-311G(d,p) level of theory are summarized in Supporting Information (Figure S2). All CHNO isomers exhibit planar geometry in their $^1A'$ ground state. The computed structure of the cyclic oxazirene isomer corresponds to the formylnitrene open structure because the N–O bond distance is too long (1.792 Å). Attempts to locate the oxazirene structure as a local minimum in the PES were unsuccessful because for any starting geometry the stationary point converged to the formylnitrene structure. We have also found in the PES a local minimum corresponding to the cyclic isomer oxaziridinylidene, **15** (Figure S2, Supporting Information), which adopts a non-planar geometry with the N heteroatom being pyramidal (the ∠H–N–C–O dihedral angle is equal to 93.7°). A planar oxaziridinylidene structure, **16TS** (Figure S2, Supporting Information), corresponds to a transition state for the inversion process of the pyramidal N heteroatom, the inversion barrier being equal to 17.95 kcal/mol. In general terms, the computed structures of the CHNO isomers are in excellent agreement with available theoretical data.[4-10,30-34]

The relative stability of CHNO isomers (Figure S2, Supporting Information) with respect to the more stable isocyanic acid computed at the B3LYP/6-311G(d,p) follows the trend predicted previously by Mebel et al.[9] at the same level of theory as well as by the more sophisticated G2 calculations.[10] Most important is the close agreement (generally within 3.6 kcal/mol) of the B3LYP/6-311G(d,p) relative stabilities to the G2 ones, which are 25.4, 70.1, and 83.8 kcal/mol for cyanic, fulminic, and isofulminic acids, respectively. We have also calculated the relative stabilities at the CCSD(T)/6-311++G(2d,p) level and found the values of 24.21, 70.01, 82.12, 85.23, and 107.04 kcal/mol for isomers **2**, **3**, **4**, **5**, and **15**, respectively. It can be seen that the CCSD(T)/6-311++G(2d,p) relative stabilities of CHNO isomers, following the same trend, are in closer agreement (generally within 1.7 kcal/mol) to the G2 ones.

The negative net atomic charge is accumulated on the N and O atoms in isomers **1**, **2**, **5**, and **15**, on the C and O atoms in **4** and only on the O atom in **3**. Obviously, these centers compose the nucleophilic centers of the isomers toward electrophiles, such as Cu^+ ions. In isofulminic acid, the negative net atomic charge on the C atom is very small. The same is also true for the N atom bearing very small positive net atomic charge. Therefore, both atoms could be considered as almost neutral, consistent with a carbene-like structure for isofulminic acid. On the other hand, the charge distribution on the N and O atoms of fulminic acid reveals the presence of a σ dative N → O bond characteristic of nitrile oxides.

The sequence of MOs deduced for all CHNO isomers is $...(7a')^2(1a'')^2(8a')^2(9a')^2(2a'')^2$. The HOMO of all isomers exhibiting a'' symmetry corresponds to doubly degenerate π-type molecular orbitals delocalized on the entire nuclear skeleton. They are constructed from the linear combination of p AOs of C, N, and O atoms, being in-phase for the C and N atoms and out-of-phase for the O atom. It should be noted that the bonding component of the HOMOs is much stronger than the antibonding one. The LUMO of CHNO isomers, except those of **2** and **4**, exhibiting a' symmetry corresponds to doubly degenerate π^*-type MOs delocalized on the entire nuclear skeleton. They are constructed from the antibonding combination of p AOs of C, N, and O atoms. In isomers **2** and **4**, the analogous π^*-type MOs correspond to LUMO+1, while their LUMOs exhibiting also a' symmetry correspond to antibonding orbitals localized mainly on the H atoms. The nature of the frontier molecular orbitals of the CHNO isomers reveals that electrophilic attack of the isomers would be expected to occur at the CN bonds, where the HOMO has its higher component, while nucleophilic attack would take place at the H atoms, where the LUMO has its higher component. The HOMO–LUMO energy gap is equal to 7.32–8.44 eV for isomers **1–4**, 6.22 eV for **15**, and 4.29 eV for **5**. The lower HOMO–LUMO energy gap of **5** suggests that a triplet state could possibly be the ground state of formylnitrene. In effect, B3LYP/6-311G(d,p) calculations indicated that the triplet state ($^3A''$) of formylnitrene, (structure **19**, Figure S2, Supporting Information) exhibiting an open-chain structure, is a local minimum in the PES at 9.02 kcal/mol lower in energy than the singlet state. It should be noted that the optimized structural parameters are in good agreement with those computed earlier[10b] at the MP2/6-31G(d) level as well as at the SCF and GVB levels.[31] Surprisingly, according to G2, the $^3A''$ state is 2.9 kcal/mol above the $^1A'$ state of formylnitrene.[10b] However, calculations of the energy separation of these two states at the more sophisticated CASPT2/cc-pVTZ//CASSCF/cc-pVDZ and QCISD(T)/cc-pVTZ//CASSCF/cc-pVDZ levels placed the triplet below the singlet state by 3.5 and 0.7 kcal/mol, respectively.[10a] The $^3A''$ state is also the ground state of formylnitrene at the SCF and GVB level.[31]

Infrared Spectra. The predicted harmonic vibrational frequencies of the CHNO isomers along with the assignment of their normal vibrational modes are listed in Supporting Information (Table S7). The experimental fundamentals of isomers **1–4** in the gas phase and in argon matrixes[5,35-38] have also been included in Table S7. Despite the large number of papers devoted to the theoretical investigation of the global potential energy surfaces of the CHNO isomers,[4-10] only a few[5,7,35] deal with the calculation and assignment of their harmonic vibrational frequencies. In general terms, the computed harmonic vibrational frequencies at the B3LYP/6-311G(d,p) level of theory are in good agreement with the experimental fundamentals.

For isocyanic acid, only five of the six fundamentals were found in argon matrixes. Notice the excellent agreement of the computed low-frequency normal modes to the experimental ones, the deviation being less than 2%. For the high-frequency normal modes assigned to ν_{asym}(NCO) and ν(NH) stretching vibrations, the deviation is larger amounting to 4%−5%. The same is also true for the low- and high-frequency vibrational bands of cyanic acid.

Fulminic acid is of special interest because its bending vibrational modes and particularly the δ(HCN) band are strongly dependent on the nature of the matrixes. In HCN and *n*-hexane matrixes at 80 K, no vibrational bands were observed[37] below 500 cm^{-1}. On the other hand, Bondybay et al.[38] have identified bands at 243 cm^{-1} (in argon matrix) and 239 cm^{-1} (in neon matrix), but their intensities were not given and the IR spectrum is only shown to 400 cm^{-1}. Moreover, Maier et al.[5] have measured the spectrum of fulminic acid, isolated in an argon matrix at 10 K, with a resolution of 0.5 cm^{-1} and also found a band at 243.6 cm^{-1}, but this band was attributed to instrumental artifact. Among the three bands observed below 600 cm^{-1}, the broader one was assigned to δ(HCN). According to our calculations, the band at 241.3 cm^{-1} is definitely assigned to δ(HCN). It is important to note the excellent agreement of the computed δ(HCN) to those found by Bondybay et al.[38] in argon and neon matrixes and the band attributed to instrumental artifact by Maier et al.[5]

For isofulminic acid, the agreement between calculated and observed bands is only fair. The frequency of the ν(OH) band is 7.6% higher than the experimental one but close to the corresponding band in the IR spectra of substituted formoximes (around 3600 cm^{-1}). The ν(NC) band occurs in isofulminic acid 178.1 cm^{-1} lower than in cyanic acid, indicating that the NC bond acquires a double bond character. The computed ν(NC) frequency is only 0.8% higher than the experimental one. The largest discrepancies between theory and experiment are in the ν(NO) and the bending vibrations. Thus, the computed ν(NO) stretching vibration is 35.8% higher than the experimental one, but the theoretical frequency seems to be more reasonable because ν(NO) stretching vibrations are expected to occur at around 900 cm^{-1}. Notice that, in formoxime,[39] it lies at 888 cm^{-1} and in hydroxylamine[40] at 895 cm^{-1}. Compare also the ν(N−O) stretching vibrational frequency of isofulminic acid to the corresponding band of the hfaox conformers appearing in the region of 920−1007 cm^{-1}. For the α' and α'' δ(ONC) vibrations, the computed frequencies are 39.6% and 19.2% lower than the experimental ones. The large discrepancy between calculated and observed bands suggests a more precise measurement of the IR spectrum of isofulminic acid in the gas phase.

The assignment of the bands in formylnitrene was based on the comparison of the computed frequencies of the singlet and triplet states. Thus, the ν(CH) stretching vibration of the singlet state at 3181.8 cm^{-1} is shifted to lower wavenumbers in the triplet state as a result of the weakening of the C−H bond. The variations of the ν(CO) and ν(CN) stretching vibrations between the singlet and triplet states follow the variations of both the bond lengths and bond overlap populations of the respective bonds in the two states. The stretching vibrational frequency of the CN bond decreases by 679.5 cm^{-1} with respect to the corresponding vibration of cyanic acid. This is not an unexpected result because the CN bond in formylnitrene is close to a double bond while in cyanic acid it is close to a triple bond. The ν(CO) stretching vibration at 1331.8 cm^{-1} is indicative of a carbonyl C=O bond exhibiting a partially double bond character.

TABLE 2: The GIAO/B3LYP/6-311+(2df,2p)//B3LYP/ 6-311G(d,p) ^{13}C, ^{14}N, ^{17}O, and ^{1}H Chemical Shifts (δ, ppm)^{a} for the CHNO Isomers

species	^{13}C	^{14}N	^{17}O	^{1}H
HNCO, **1**	141.6	28.9	146.0	2.6
HOCN, **2**	119.8	183.9	37.1	3.6
HCNO, **3**	24.7	216.8	126.5	2.1
HONC, **4**	130.5	182.7	133.9	5.4
formylnitrene, **5**	182.9	657.8	214.5	10.5
oxaziridinylidene, **15**	293.0	173.9	315.8	2.7

^{a} The external reference standards used for the ^{13}C, ^{14}N, ^{17}O, and ^{1}H NMR spectra were the CH$_4$, NH$_3$, H$_2$O, and TMS molecules, respectively.

Finally, for the oxaziridinylidene isomer, the expected six fundamentals have been identified. The ν(NH) stretching vibration is shifted to lower wavenumbers (198 cm^{-1}) with respect to the corresponding frequency of isocyanic acid. On the other hand, the ν(CO) stretching vibration is shifted to higher wavenumbers (167 cm^{-1}) with respect to the corresponding frequency of the formylnitrene isomer. The same is also true for the ν(NO) stretching vibration, which is shifted by about 211 cm^{-1} toward higher wavenumbers with respect to the corresponding band of the isofulminic isomer.

NMR Spectra. The ^{13}C, ^{15}N, ^{17}O, and ^{1}H chemical shifts (δ, ppm) in the NMR spectra of CHNO isomers calculated at the GIAO/B3LYP/6-311++G(2d,p)//B3LYP/6-311G(d,p) level of theory are given in Table 2. The calculated absolute shielding tensor elements (σ, ppm) are summarized in Supporting Information (Table S8). Notice that the computed NMR spectra of CHNO isomers are predictions because there are no experimental data available so far.

The fulminic acid has the lower ^{13}C chemical shift ($\delta = 24.7$ ppm), and oxaziridinylidene has the higher one ($\delta = 293.0$ ppm.). Obviously, the high shielding of the C atom in fulminic acid is the result of its bonding characteristics, being an sp-hybridized C atom triply bonded to a N atom. This is substantiated upon comparing the computed ^{13}C chemical shift of isofulminic acid to that of HCN computed at various levels of theory.[41] The high shielding of the C atom in fulminic acid could be attributed to the high anisotropic shielding characterizing the linear π systems.[42] In the framework of the analysis given by Pople,[42] when the molecular axis is aligned parallel to the applied magnetic field, there is only a diamagnetic contribution, σ^d, to the magnetic shielding. For symmetry reasons, the paramagnetic contribution, σ^p, to the magnetic shielding is zero. In that case, the shielding along the molecular axis is much higher than that perpendicular to the axis, and therefore, the total isotropic shielding, σ^{iso}, is increased. This explanation was substantiated by the observed ^{13}C and ^{15}N chemical shifts in a series of compounds determined experimentally by solid state and liquid crystal NMR spectroscopy[43,44] as well as by means of ab initio quantum chemical techniques.[45] The small bending of the OCN moiety in cyanic acid accounts for the deshielding of the C atom with respect to that of fulminic acid. On the other hand, the high deshielding of the C atom in oxaziridinylidene is reflected on its bonding characteristics, being an sp^3-hybridized C atom singly bonded to a N atom (compare the bond overlap population of the respective bonds). Finally, isomers **1**, **4**, and **5** exhibit ^{13}C chemical shifts in the range of 130.5−182.9, being expected for a nearly sp^2-hybridized C atom doubly bonded to a N atom. It can be seen that ^{13}C NMR spectroscopy can be used to distinguish fulminic acid and formylnitrene, the two possible dehydration products of the most stable (Z)-(s-cis,s-trans) hfaox conformer.
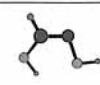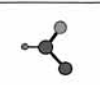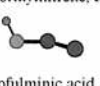
Ab Initio Quantum Chemical Study

J. Phys. Chem. A, Vol. 106, No. 7, 2002 **1431**
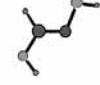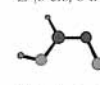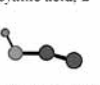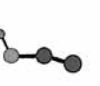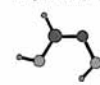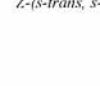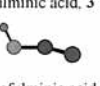
The isocyanic acid has the lower ^{15}N chemical shift (δ = 28.9 ppm), and formylnitrene has the higher one (δ = 657.8 ppm). In the isomers **2**, **3**, **4**, and **15**, the ^{15}N chemical shifts were found in the range of 173.9−216.8. The high shielding of the N atom in isocyanic acid is due to both its high electron density and the nearly linear NCO moiety. The strong deshielding effect observed for the ^{15}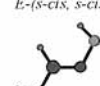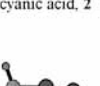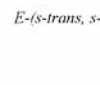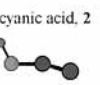N chemical shift of the linear fulminic acid might be due to the low electron density on the N atom (the N atom acquires positive net atomic charge). The linearity along with the electron density distribution and bonding features could account for the computed ^{15}N chemical shifts of isomers **2**, **3**, **4**, and **15**.

The cyanic acid has the lower ^{17}O chemical shift (δ = 37.1 ppm), and oxaziridinylidene has the higher one (δ = 315.8 ppm.). Similar arguments could also explain the observed ^{17}O chemical shift of CHNO isomers. Generally, the terminal O atom in a −NCO moiety shows a shielding effect with respect to other carboxylic O atoms,[46] amounting to about 200 and 400 ppm with respect to amides and carbonyl compounds,[47] respectively, and a deshielding effect only toward the isoelectronic CO_2 molecule.[48] It is important to note that the atoms showing the highest shielding effects in CHNO isomers are those bonded to the hydrogen atom and therefore the H atom should be the key factor for the high shielding of the atoms to which it is bonded.

Finally, the ^{1}H chemical shifts are found in the range of 2.1−10.5 ppm. The higher deshielding of the H atom in formylnitrene could probably be due to its lower electron density. In general terms, the ^{1}H chemical shifts are dependent on the nature of the atom with which it is bonded.

Heats of Dehydration Reactions of Hydroxyformaldoxime Conformers. The heats of dehydration reactions ($\Delta_R H$) of hfaox conformers computed at the B3LYP/6-311G(d,p) level of theory are listed in Table 3. All dehydration processes, except those yielding cyanic acid, are predicted to be endothermic. The most endothermic one is the dehydration reaction of the more stable (*Z*)-(*s*-cis,*s*-trans) conformer, **7**, to formylnitrene, with the computed heat of reaction being equal to 51.34 kcal/mol. On the other hand, the most exothermic dehydration process is the dehydration reaction of the (*E*)-(*s*-trans,*s*-cis) conformer, **14**, to cyanic acid with the computed heat of reaction being equal to −26.16 kcal/mol. All dehydration processes yielding cyanic acid are exothermic, while those yielding formylnitrene, fulminic acid, or isofulminic acid are endothermic. Notice that isocyanic acid could not be a direct dehydration product of hfaox conformers. Obviously, aqueous solutions of formylnitrene, fulminic acid, and isofulminic acid might be expected to contain significant amounts of hfaox conformers. The reaction pathway for the addition of water to fulminic acid is predicted to occur via the transition state **20TS** with an activation barrier of 68.18 kcal/mol at the B3LYP/6-311G(d,p) level (Figure 2). The imaginary frequency at 1464i cm^{-1} corresponds to vibration mainly along the forming H···ON bond. Intrinsic reaction paths were traced from the **20TS** structure on either side of the saddle point to make sure that no further intermediates exist. The structure of **20TS** differs from that reported previously[13] because it corresponds to a more synchronous mechanism. The O−H bond-breaking and O−H bond-forming processes are almost synchronous in the transition state with proton transfer taking place at the TS. This could account for the much higher activation barrier computed at the B3LYP/6-311G(d,p) level with respect to that of 31.5 kcal/mol computed at the HF/6-31G* optimized geometry of a reactant-like transition state. The formation of the transition state involves as a first step the

TABLE 3: Heats of Reactions, $\Delta_R H$ (kcal mol^{-1}), for Dehydration Reactions of Hydroxyformaldoxime Conformers Computed at the B3LYP/6-311G(d,p) Level of Theory

Hydroxyformaldoxime conformer	CHNO isomer	$\Delta_R H$(kcal/mol)
Z-(*s*-cis, *s*-trans), 7	formylnitrene, 5	51.34
	isofulminic acid, 4	46.86
E-(*s*-cis, *s*-trans), 8	cyanic acid, 2	-14.96
Z-(*s*-trans, *s*-trans), 9	isofulminic acid, 4	40.10
E-(*s*-trans, *s*-trans), 10	isofulminic acid, 4	38.93
Z-(*s*-trans, *s*-cis), 11	fulminic acid, 3	19.54
	isofulminic acid, 4	38.67
E-(*s*-cis, *s*-cis), 12	cyanic acid, 2	-20.53
E-(*s*-trans, *s*-cis), 14	cyanic acid, 2	-26.16
	isofulminic acid, 4	32.47

deformation of fulminic acid. In the *E*-trans mode, the water approaches the electrophilic carbon atom; this determines that the product will have the *Z*-configuration, as experimentally observed in all analogous reactions.[49] The second step involves the transfer of one of the H atoms of the water molecule to the O atom of the deformed fulminic acid with the concomitant formation of the C−O bond, thus leading to the hfaox conformer with the (*Z*)-(*s*-trans) configuration. It should be noted that the hfaox conformer formed is the (*Z*)-(*s*-trans,*s*-cis) conformer, **11**, in line with the previously reported results,[12,13] which further isomerizes to the more stable (*Z*)-(*s*-cis,*s*-trans) conformer **7** via **13TS** (Figure 2). A comparison of the net atomic charges and bops of **20TS** (Figure 2) to those of **11** reveals that an anticlockwise cyclic electron delocalization occurs from the O atom of the approaching water molecule toward the C atom of the highly deformed fulminic acid. Most of the delocalized electron density in **20TS** is withdrawn from the C atom and accumulated on the N atom, thus resulting in the reinforcement of the C−N bond in the final product **11**. On the whole, the B3LYP/6-311G(d,p) results confirm the previous predictions[12,13] that the addition of water to fulminic acid is concerted. The computed B3LYP/6-311G(d,p) heat of reaction for the addition of water to fulminic acid amounting to −19.54 kcal/mol
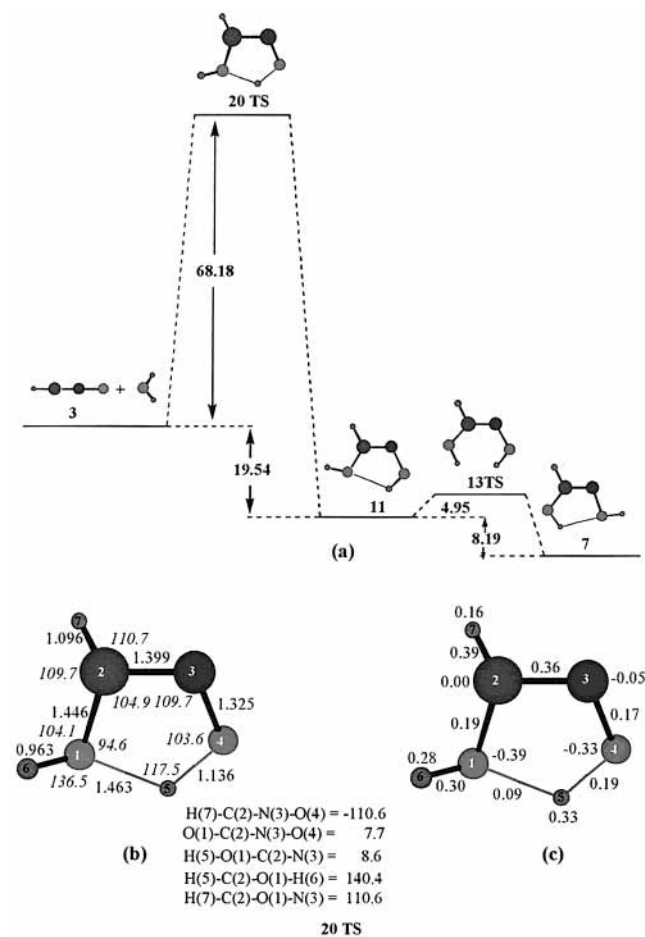
Figure 2. Energetic (kcal/mol) and geometric profile of the nucleophilic addition of water to fulminic acid computed at the B3LYP/6-311G(d,p) level of theory (a); the structural parameters (bond lengths in Å, bond angles in deg) (b), and Mulliken net atomic charges and bond overlap populations (figures in italics) of transition state **29TS** (c.)
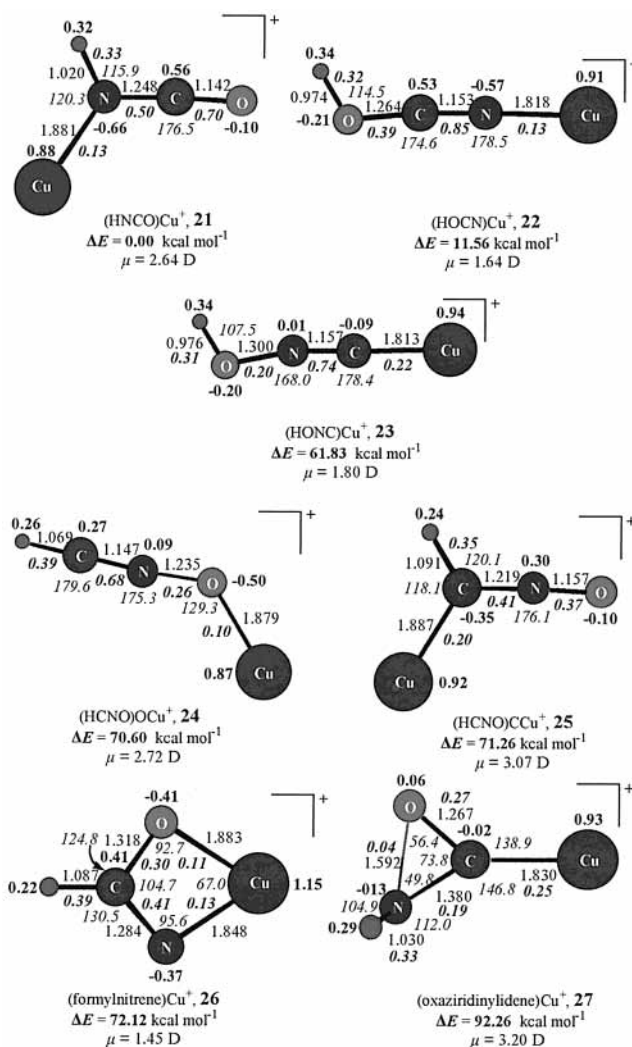

Figure 3. Equilibrium structures (bond lengths in Å, bond angles in deg), relative stability (in kcal), and dipole moments of the Cu$^+$ complexes of the CHNO isomers computed at the B3LYP/6-311G(d,p) level of theory.

compares well with the previously[13] estimated value of −23.9 kcal/mol including Δ*E* (MP4/6-31G(d,p) and ZPEs.

Coordination of CHNO Isomers to Cu$^+$ Ions. The interaction of Cu$^+$ ions with the CHNO isomers was analyzed in the framework of DFT theory. The equilibrium structures of the Cu$^+$ complexes of the CHNO isomers, along with the net atomic charges, bond overlap populations, relative stability, and dipole moments computed at the B3LYP/6-311G(d,p) are summarized in Figure 3.

Calculated Structures, Relative Stabilities, and Bonding. Perusal of Figure 3 shows that, with the only exception of the Cu$^+$ complex of isofulminic acid, the relative stability of the complexes follows that of the respective free ligands. In both the (HNCO)Cu$^+$, **21**, and (HOCN)Cu$^+$, **22**, complexes, the Cu$^+$ ions show a selective binding to the N donor atoms. Notice that the N donors atoms have the higher negative net atomic charge in both the HNCO and HOCN isomers. Attachment of Cu$^+$ ions to O donor atoms, being also negatively charged, seems to be impossible. All attempts to identify a stationary point in the PES corresponding to HNCO−Cu$^+$ and HO(Cu$^+$)CN complexes failed, even starting with the computed geometry of the HNCO−Cu$^+$ complex at the same level of theory reported recently.[50] This may be due to higher convergence criteria used in our calculations with respect to those normally used in the Gaussian program suite. With these convergence criteria, the total electronic energy of the free Cu$^+$ ion was found to be 2.17 × 10^{-4} hartree lower than that computed using the default

convergence criteria of the Gaussian program.[51] The preference of both HNCO and HOCN isomers to be coordinated to the Cu$^+$ ion through the N donor atom is not an unexpected result because their HOMO and HOMO−1, being the donor orbitals, are primarily localized on the N atom. Interestingly, upon coordination of HNCO and HOCN to Cu$^+$ ions, there is a significant increase of the negative net atomic charge of the N donor atoms as a result of the strong inductive effect of the Cu$^+$ ions. This is also reflected in the increase of the positive net atomic charge of the H atoms, thus exhibiting higher acidic character. The induced charge redistributions are mirrored on the net atomic charges of all other atoms as well as on the bond overlap populations and bond lengths. The C−N bonds directly affected by coordination are significantly activated, while concomitantly the N−O bonds are reinforced upon coordination in both complexes. Notice that the Cu−N coordination bond is stronger in complex **22** than that in **21** (compare the calculated bond lengths) in line with the computed interaction energies, being 65.31 and 48.23 kcal/mol, respectively. Surprisingly, the Cu−N bond overlap populations are in reverse order with respect to the bond lengths and interaction energies, thus suggesting that the ionic component has a significant contribution in the Cu−N bonding. In complex **22**, the charge transferred to the Cu$^+$ ion is only 0.09 charge unit, while in **21**, it is much higher amounting to 0.22 charge unit.

Isofulminic acid prefers to coordinate with Cu^+ ion only through the terminal C donor atom, as expected from the nature of its HOMO and HOMO−1 donor orbitals, which are mainly located on that atom. Attempts to identify a stationary point in the PES corresponding to a $HO(Cu^+)NC$ complex with attachment of the Cu^+ ion at the O donor atom bearing the higher negative net atomic charge failed. The Cu−C bond in the $HO(Cu^+)NC$ complex is predicted to be stronger than the Cu−N bonds in $HN(Cu^+)CO$ and $HOCNCu^+$ complexes, the Cu−C interaction energy being 73.68 kcal/mol. Surprisingly, attachment of Cu^+ ion at the C donor atom of HONC ligand does not lead to significant charge redistributions. The charge transferred to the Cu^+ ion is only 0.06 charge unit. Moreover, in contrast to $HN(Cu^+)CO$ and $HOCNCu^+$ complexes, the C−N bond in **23** directly affected by coordination is significantly reinforced (the bop of the complex is 0.742 as compared to the 0.475 value of the free ligand), while all other bonds, except the H−O bond, are only slightly reinforced upon coordination. The bop value of 0.745 indicates that upon coordination of isofulminic acid the C−N bond becomes closer to a triple bond analogous to those existing in cyanic and fulminic acids. This is substantiated from the linearity of the Cu−C−N moiety, compatible with an sp-hybridized C atom. Moreover, the charge distribution in complex **23** reveals that the Cu−C bond exhibits a higher covalent character than the Cu−N bond in complexes **21** and **22**.

Fuminic acid acts as an ambidentate ligand via either the C or O donor atoms as expected from the nature of its HOMO and HOMO−1 donor orbitals having nearly equivalent components on both atoms. Attempts to identify a stationary point in the PES corresponding to a bidentate η^2-C,O bonding of HCNO ligand forming with Cu^+ ion a four-member chelate ring failed. The attachment of the Cu^+ ion at the O donor atom of HCNO was found to be slightly more stable than the attachment at the C donor atom by only 0.66 kcal/mol. The computed interaction energies for the Cu···O and Cu···C interactions are 45.78 and 45.13 kcal/mol, respectively. Attachment of the Cu^+ ion at the C or O donor atoms of the HCNO ligand leads to significant charge redistributions. The bonds directly affected by coordination, the N−O and C−N bonds in $HCNO−Cu^+$ and $HC(Cu^+)NO$ complexes, respectively, are significantly activated, while concomitantly the C−N and N−O in the respective complexes are reinforced upon coordination in both complexes. In both complexes, the C−H bonds are weakened upon coordination. The charge transferred to the Cu^+ ion is 0.13 and 0.08 charge unit in $HCNO−Cu^+$ and $HC(Cu^+)NO$ complexes, respectively. Interestingly, in $HC(Cu^+)NO$, the C donor atom acquires high negative net atomic charge, and the same is also true for the O donor atom in the $HCNO−Cu^+$ complex.

Formylnitrene is the only CHNO isomer forming with Cu^+ ion a four-member chelate ring with the Cu−N bond a little stronger than the Cu−O one. The interaction energy was found to be 67.86 kcal/mol. It is worth noting that in complex **26** a charge transfer occurs toward both the O and N donor atoms following two different pathways. The first pathway involves the charge transfer from the Cu^+ ion, which loses 0.15 charge unit, and the second one involves the charge transfer from C and H atoms to the donor atoms increasing the positive net atomic charge of the C and H atoms by 0.12 and 0.09 charge unit, respectively. Both the C−N and C−O bonds directly affected by coordination are significantly activated, while the ∠O−C−N bond angle is opened by 15.6°. Obviously, the nonisolable formylnitrene isomer readily collapsing to the more

stable CHNO isomers could be stabilized upon coordination with a Cu^+ ion.

Finally, the oxaziridinylidene ligand is selectively coordinated to the Cu^+ ion through the C donor atom, which is more contributing to the HOMO. The computed interaction energy of 68.00 kcal/mol compares well to that of isofulminic acid, in line with the similar bonding modes of the two ligands to Cu^+ ions. Attachment of the Cu^+ ion at the C donor atom of the oxaziridinylidene ligand strengthens significantly both the C−O and C−N bonds directly affected by coordination, while concomitantly the N−O bond is weakened. Because of the charge redistribution resulting from coordination of the ligand, the O donor atom acquires a positive net atomic charge. Moreover, the charge transferred to the Cu^+ ion amounts to 0.07 charge unit.

Infrared Spectra. The predicted harmonic vibrational frequencies of the Cu^+ complexes of the CHNO ligands along with the assignment of their normal vibrational modes are listed in detail in the Supporting Information (Table S9). We will only analyze the most characteristic features of the infrared spectra of the complexes in comparison to those of the free ligands. In general terms, all observed shifts of the vibrational frequencies resulted from the association of the Cu^+ ion with the CHNO isomers are in line with both the observed structural and charge distribution changes introduced by the coordination.

Upon attachment of the Cu^+ ion at the N atom of isocyanic acid, the $\nu(NH)$ frequency appears shifted 181 cm^{-1} to the red. The same is also true for the $\delta(HNC)$ frequency, which is red-shifted by 420 cm^{-1}. The $\nu_{asym}(NCO)$ is shifted 9 cm^{-1} to the red, while the $\nu_{sym}(NCO)$ is blue-shifted by 29 cm^{-1}. A red shift is also observed for the $\nu(OH)$ frequency in the $HOCN−Cu^+$ complex amounting to 75 cm^{-1}, while both the $\nu(CN)$ and $\nu(CO)$ are blue-shifted by 75 and 114 cm^{-1}, respectively. Of special importance is the strong red-shift of both the $\nu(CH)$ and $\nu_{asym}(CNO)$ frequencies in the $HC(Cu^+)NO$ positional isomer by 489 and 160 cm^{-1}, respectively. In the other positional isomer, $HCNO−Cu^+$, the observed shifts of the bands are smaller. Thus, the $\nu(CH)$ frequency is red-shifted by only 80 cm^{-1}, while the $\nu_{asym}(CNO)$ and $\nu_{sym}(CNO)$ become separated as pure $\nu(CN)$ and $\nu(NO)$ vibrations at 2348 and 1212 cm^{-1}, respectively. In the Cu^+ complex of isofulminic acid, the $\nu(OH)$ frequency is red-shifted by 71 cm^{-1}, while the $\nu(CN)$ frequency is blue-shifted by 143 cm^{-1}. Moreover, the $\nu(NO)$ frequency is also red-shifted by 115 cm^{-1}. The coordination of Cu^+ ion to the bidentate formylnitrene ligand introduces a red shift in both the $\nu(CN)$ and $\nu(NO)$ vibrations by 159 and 36 cm^{-1}, respectively, while the $\delta(ONC)$ vibration is blue-shifted by about 260 cm^{-1}. Finally, the attachment of the Cu^+ ion to the C atom of oxaziridinylidene results in a blue-shift of $\nu(CO)$ and $\nu(CN)$ vibrations by 113 and 192 cm^{-1}, respectively, while the $\nu(NO)$ vibration is red-shifted by about 53 cm^{-1}.

NMR Spectra. The ^{13}C, ^{15}N, ^{17}O, ^1H, and ^{29}Cu chemical shifts (δ, ppm) in the NMR spectra of $(CHNO)Cu^+$ complexes calculated at the GIAO B3LYP/6-311+G(2df,2p) level of theory using the B3LYP/6-311G(d,p) optimized geometries are given in Table 4. The calculated absolute isotropic shielding tensor elements (σ, ppm) are summarized in Supporting Information (Table S10).

Generally, the association of Cu^+ ion with the CHNO isomers has, as expected, a deshielding effect on the coordinated donor atom, while all other atoms are shielded. In complex **21**, the N donor atom is deshielded by 18 ppm, while the terminal O atom exhibits an unexpectedly high shielding by 115.5 ppm. The N donor atom in complex **22** shows a stronger deshielding effect

TABLE 4: The GIAO/B3LYP/6-311+(2df,2p)//B3LYP/6-311G(d,p) ^{13}C, ^{14}N, ^{17}O, and ^{1}H Chemical Shifts (δ, ppm)^a for the Complexes of CHNO Isomers with Cu$^+$ Ions

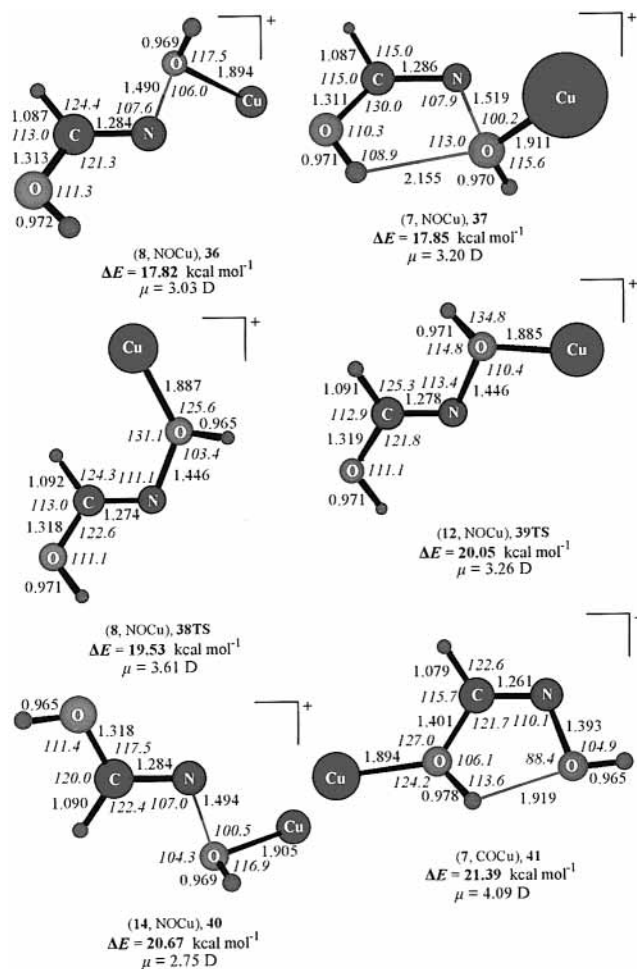| species^b	^{13}C	^{14}N	^{17}O	^{1}H
(HN**C**O)Cu$^+$, **21**	151.5	10.9	230.5	4.4
(HO**C**N)Cu$^+$, **22**	121.0	109.1	44.5	5.8
(HON**C**)Cu$^+$, **23**	98.6	192.2	133.8	6.9
(H**C**NO)Cu$^+$, **24**	51.7	193.3	74.3	4.0
(H**C**NO)Cu$^+$, **25**	25.3	377.5	460.9	5.9
(formylnitrene)Cu$^+$, **26**	684.2	231.0	180.7	11.7
(oxaziridinylidene)Cu$^+$, **27**	247.0	231.0	319.2	6.6

^{a} The external reference standards used for the ^{13}C, ^{14}N, ^{17}O, and ^{1}H NMR spectra were the CH$_4$, NH$_3$, H$_2$O, and TMS molecules, respectively. ^{b} The atoms in bold are the donor atoms in the complexes.
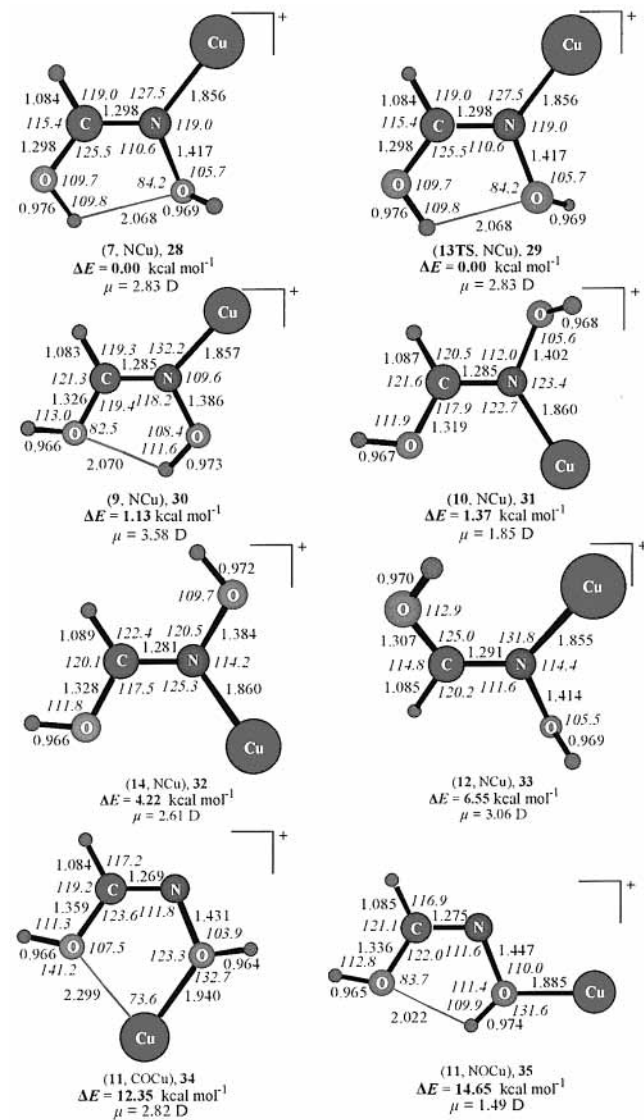
Figure 4. Equilibrium structures (bond lengths in Å, bond angles in deg), relative stability (in kcal), and dipole moments of Cu$^+$ complexes of the hfaox conformers computed at the B3LYP/6-311G(d,p) level of theory.

Figure 5. Equilibrium structures (bond lengths in Å, bond angles in deg), relative stability (in kcal), and dipole moments of Cu$^+$ complexes of the hfaox conformers computed at the B3LYP/6-311G(d,p) level of theory.

by 74.8 ppm. The attachment of Cu$^+$ ion to the C donor atom of isofulminic acid in **23** deshields the donor atom by 31.9 ppm, while the rest atoms of the complex are weakly shielded. Coordination of the Cu$^+$ ion to the O donor atom of fulminic acid results in the deshielding of both the O donor and the neighboring N atoms by 52.2 and 23.5 ppm, respectively, while the C and H atoms are shielded by 27.0 and 1.9 ppm, respectively. On the other hand, coordination of the Cu$^+$ ion to

the C donor atom of fulminic acid introduces a shielding effect to all atoms, which is surprisingly very strong for the non-coordinated N and O atoms amounting to 179.5 and 334.4 ppm, respectively. Even the C donor atom is slightly shielded by 0.6 ppm. Most important is the strong deshielding effect on the N donor atom in complex **26** amounting to 426.8 ppm followed by a concomitant strong shielding of the C atom by 501.3 ppm. The O donor atom involved in the four-member chelate ring is only slightly deshielded by 33.8 ppm. Finally, in complex **27**, the C donor atom is deshielded by 46.0 ppm, while the neighboring N and O atoms are shielded by 57.1 and 3.4 ppm, respectively.

Coordination of Hydroxyformaldoxime Conformers to Cu$^+$ Ions. The interaction of Cu$^+$ ions with the hfaox conformers was also analyzed in the framework of DFT theory. The equilibrium structures of (hfaox)Cu$^+$ complexes corresponding to global and local minima in the PES along with the relative stability and dipole moments computed at the B3LYP/6-311G(d,p) are summarized in Figures 4–6. Moreover, by searching the conformational space of (hfaox)Cu$^+$ complexes, a number of transition states were also located on the PES with their structures, relative stabilities, and dipole moments included also in Figures 5 and 6. The hfaox ligands, disposing three donor atoms, could be coordinated to the Cu$^+$ ion according to the following bonding modes: (i) through the N donor atom, (ii) through the O donor atoms in a unidentate bonding mode, and (iii) through the O donor atoms in a bidentate bonding mode.
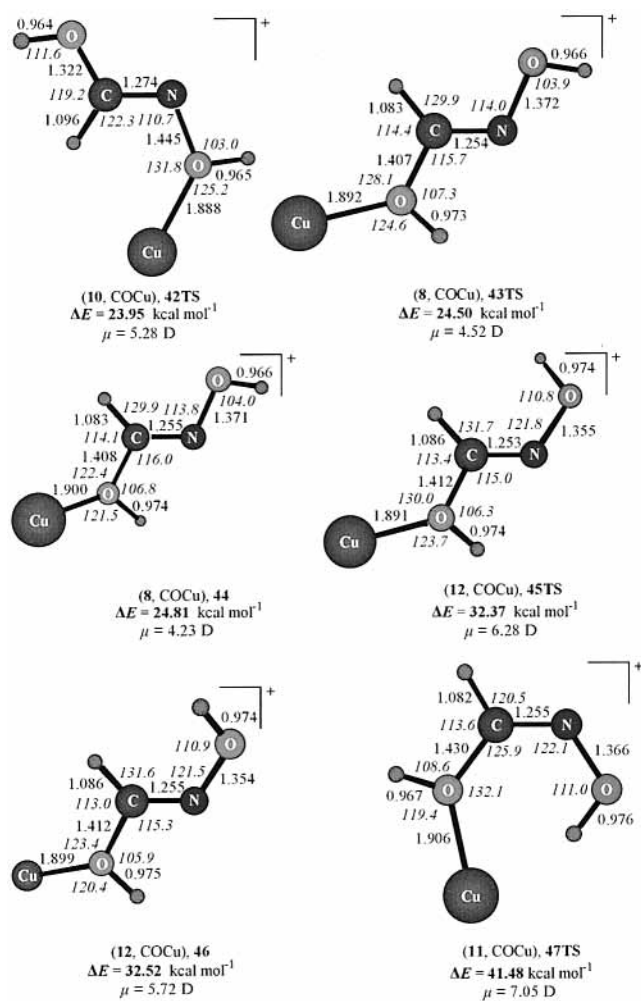
Ab Initio Quantum Chemical Study

J. Phys. Chem. A, Vol. 106, No. 7, 2002 **1435**

Figure 6. Equilibrium structures (bond lengths in Å, bond angles in deg), relative stability (in kcal), and dipole moments of Cu⁺ complexes of the hfaox conformers computed at the B3LYP/6-311G(d,p) level of theory.

TABLE 5: Interaction Energies (kcal/mol) of Cu⁺ Ions with Hydroxyformaldoxime Conformers for All Possible Bonding Modes Computed at the B3LYP/6-311G(d,p) Level of Theory

conformer	complex	interaction energy
(Z)-(s-cis,s-trans), **7**	**7**, NCu, **28**	62.61
	7, NOCu, **37**	44.75
	7, COCu, **41**	41.22
(Z)-(s-trans,s-trans), **9**	**9**, NCu, **30**	68.14
	9, NOCu, **34**	57.03
	9, COCu, **34**	57.03
(Z)-(s-trans,s-cis), **11**	**11**, NCu, **30**	69.67
	11, NOCu, **35**	56.15
	11, COCu, **34**	58.46
(Z)-(s-cis,s-cis), **13TS**	**13TS**, NCu, **29**	75.29
	13TS, NOCu, **37**	57.43
	13TS, COCu, **41**	53.90
(E)-(s-cis,s-trans), **8**	**8**, NCu	
	8, NOCu, **36**	47.97
	8, COCu, **44**	40.98
(E)-(s-trans,s-trans), **10**	**10**, NCu, **31**	69.16
	10, NOCu, **31**	69.16
	10, COCu, **31**	69.16
(E)-(s-cis,s-cis), **12**	**12**, NCu, **33**	64.80
	12, NOCu, **39TS**	51.30
	12, COCu, **46**	38.84
(E)-(s-trans,s-cis), **14**	**14**, NCu, **32**	72.77
	14, NOCu, **40**	56.32
	14, NCu, **32**	72.77

Perusal of Figures 4−6 illustrates that the Cu⁺ ions show a higher affinity for the N donor atom followed by the O donor atom of the oxime (−NOH) group and the O donor atom of the C−OH moiety. The computed interaction energies of the Cu⁺ ion with the hfaox conformers for all possible bonding modes are collected in Table 5. The important issue of the Cu⁺ ion preference for the association with the N donor atom of hfaox ligands has been addressed to a frontier-orbital-controlled rather than to a charge-controlled mechanism because the N donor atom has much lower negative net atomic charge than the two O donor atoms. In effect, the HOMOs of the hfaox conformers involved in the formation of the dative coordination bond upon interaction with the vacant d orbitals of the Cu⁺ ion exhibit a higher component on the N donor atom. On the other hand, the charge-controlled mechanism seems to be operating in the bonding mode of the Cu⁺ ion to the O donor atoms. As can be seen in Table 5, there are some general trends and evidences common to all coordination modes, and they will be used as a starting point of the discussion.

The attachment of the Cu⁺ ion to the N donor atom of conformer **7** is 17.86 and 21.39 kcal/mol more favorable than the attachment to the O donor atoms of the −NOH and −COH moieties, respectively. Interestingly, the same is also true for the attachment of the Cu⁺ ion to the N donor atom of conformer **13TS**, which results in the formation of **29**, being the optical isomer of complex **28**, with the H atom of the −NOH moiety

pointing on each side of the molecular plane. Notice that both conformers **7** and **13TS** afford complexes **37** and **41** upon attachment of the Cu⁺ ion to −NOH and −COH moieties, respectively. The association of the Cu⁺ ion with conformer **9**, either to ON or OC donor atoms results in an η^2-bonding mode, **34**, with the interaction energy being 11.11 kcal/mol less than that for the association of the Cu⁺ ion to the N donor atom. Complex **34** is also obtained upon attachment of Cu⁺ ion to the OC donor atom of conformer **11**. The attachment of Cu⁺ ion to the N donor atom of conformers **9** and **11** affords complex **30**. Surprisingly, the COCu bonding mode is favored by 2.31 kcal/mol with respect to NOCu one upon association of Cu⁺ ion with conformer **11**. It is important to note that complex **31** is formed upon interaction of conformer **10** with Cu⁺ ion following either the trajectory of the attachment of Cu⁺ ion to the OC or the ON donor atoms. In both cases, the formation of complex **31** proceeds through the transition state **42TS** with an activation barrier of 22.33 kcal/mol. On the other hand, following the trajectory involving the attachment of the Cu⁺ ion to the N donor atom of conformer **10**, the expected complex **31** is obtained. Attempts to locate a local minimum in the PES of **8**, NCu, failed because of convergence problems of the calculations. The association of Cu⁺ ion to the ON and OC donor atoms of **8** affords **36** and **44**. The attachment of Cu⁺ ion to the N donor atom of conformer **12** is 13.50 and 25.96 kcal/mol more favorable than the attachment to the O donor atoms of the −NOH and −COH moieties, respectively. Finally, the attachment of Cu⁺ ion to the N donor atom of conformer **14** is 16.45 kcal/mol more favorable than the attachment to the O donor atom of the −NOH moiety. Surprisingly, approaching the Cu⁺ ion to the N or OC donor atoms of conformer **14** results in the attachment of Cu⁺ ion to the N donor atom (**14**, NCu, **32**).

Attachment of the Cu⁺ ion to the N donor atom of hfaox ligands leads to structural changes accompanied by significant charge redistributions as well. The net atomic charges and bops computed at the B3LYP/6-311G(d,p) level are given in Supporting Information (Figures S3 and S4).
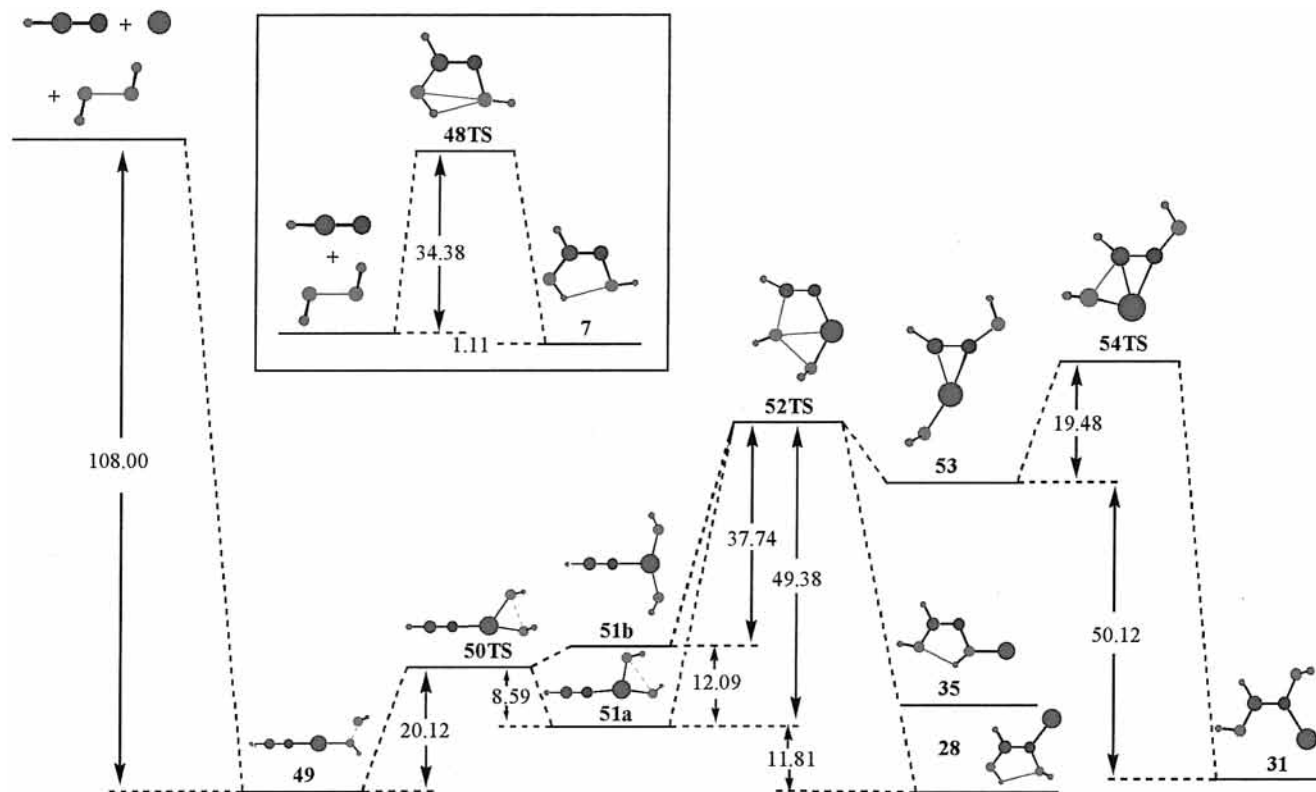
Figure 7. Energetic (kcal/mol) and geometric profile of the oxidation of organic nitriles with hydrogen peroxide to form oximes with and without the presence of Cu⁺ ions computed at the B3LYP/6-311G(d,p) level of theory.

In the NCu bonding mode, the C−N bond is lengthened by about 0.02 Å, while the N−O bond (except in complex **33**) is shortened by about 0.01 Å. In complex **33**, the N−O bond is lengthened by about 0.02 Å. The adjacent C−O bond is also reinforced upon coordination being shortened by about 0.03−0.05 Å. The charge transferred to the Cu⁺ ion is 0.14−0.18 charge unit. Interestingly, the N donor atom directly involved in the bonding acquires a significantly higher negative net atomic charge amounting to 0.2−0.3 charge unit with respect to the free ligand. The two O atoms show a smaller increase of their negative net atomic charge, while the C atom acquires a significantly higher positive net atomic charge amounting to 0.1−0.2 charge unit. The bop reflects the corresponding structural changes.

In the η^2-bonding mode, **34**, the NOCu interaction is much stronger than the COCu one as is mirrored on both the Cu−O bond distances and the bop values. The charge transferred to the Cu⁺ ion is only 0.10 charge unit. The two O donor atoms acquire higher negative net atomic charges, by 0.18 and 0.07 charge unit, respectively, while there is a small charge transfer from both the C and N atoms toward the O donor atoms.

Considering the NOCu bonding mode, it can be seen that the N−O bond is significantly activated being lengthened by about 0.03−0.10 Å, while the C−O bond is shortened by about 0.03 Å. The adjacent C−N bond is lengthened by about 0.01−0.02 Å. The charge transferred to the Cu⁺ ion is 0.11−0.13 charge unit. The O donor atom directly involved in the bonding acquires a significantly higher negative net atomic charge amounting to 0.2−0.3 charge unit with respect to the free ligand. The OC and the N atoms show a smaller decrease of their negative net atomic charge, while the positive net atomic charge of the C atom increases by 0.05−0.10 charge unit. The bop again reflects the corresponding structural changes. Notice the strong activation of the N−O bond (bop values of only 0.03−

0.07), suggesting the formation of a Cu−OH moiety weakly interacting with the rest of the hfaox molecule.

Finally, in the COCu bonding mode, the C−O bond is lengthened by about 0.6 Å, while the C−N bond is shortened by about 0.01 Å. The more distant N−O bond is also shortened by about 0.03−0.04 Å. The charge transferred to the Cu⁺ ion is 0.07−0.13 charge unit. The O donor atom directly involved in the bonding acquires a significantly higher negative net atomic charge amounting to about 0.20 charge unit with respect to the free ligand. The ON and the N atoms show a smaller decrease of their negative net atomic charge amounting to 0.02−0.09 and 0.05−0.08, respectively, while the positive net atomic charge of the C atom increases by 0.02−0.07 charge unit.

Oxidation of HCN to Hydroxyformaldoxime by Hydrogen Peroxide. The observed strong activation of the N−O and C−O bonds induced by the coordination of hfaox ligands to Cu⁺ ion prompts us to investigate further the mechanism of the respective reaction. Surprisingly, a search of possible reaction pathways revealed the formation of a mixed-ligand (hydrocyanide)(hydrogen peroxide)copper(I) complex as the final product. Therefore, we thought it would be advisable to investigate the mechanism of the reverse reaction, namely, the oxidation of HCN with hydrogen peroxide to yield hydroxyformaldoxime, and explore the role played by the Cu⁺ ions. Notice that this is a novel reaction, which could be generally used to convert organic nitriles to oximes under oxidation with hydrogen peroxide. The energy profiles of the reactions are depicted schematically in Figure 7, while the most significant geometrical parameters of all of the stationary points located on the PES governing the reaction are shown in Figure 8. The net atomic charges and bops along with additional structural parameters computed at the B3LYP/ 6-311G(d,p) level are given in Supporting Information (Figures S5 and S6). It can be seen that HCN could react with H₂O₂ to yield conformer **7** through
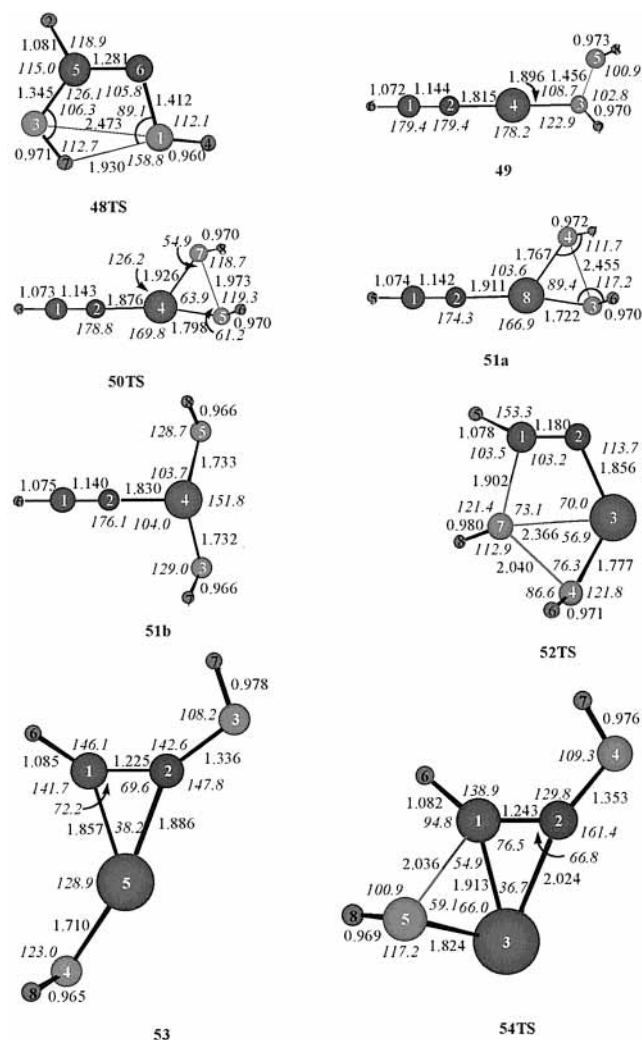
Figure 8. Equilibrium structures (bond lengths in Å, bond angles in deg) of possible species involved in the oxidation of organic nitriles with hydrogen peroxide to form oximes in the presence of Cu^+ ions computed at the B3LYP/6-311G(d,p) level of theory.

a product-like transition state, **48TS**, mirrored on both their structural and electronic parameters. The bop value of 0.001 for the O···O separation in **48TS** indicates weak bonding interactions as compared to the antibonding ones in **7** (bop = −0.013). The imaginary frequency at 203i cm^{-1} corresponds to movements of H(4) and H(7) along the z axis to reach the planarity of **7**. The oxidation of HCN by H_2O_2 to yield conformer **7** is almost thermoneutral ($\Delta_R H = -1.11$ kcal/mol) and has to surmount an energy barrier of 34.38 kcal/mol. In the presence of Cu^+ ions, the first step involves the formation of the mixed-ligand (hydrocyanide)(hydrogen peroxide)copper(I) complex, **49**, found at 108.00 kcal/mol lower in energy than the reactants. Complex **49** is transformed to **51a** through **50TS** with an activation barrier of 20.12 kcal/mol. The transformation of **49** to **51a** corresponds to an endothermic process ($\Delta_R H =$ 11.47 kcal/mol). We have also located on the PES a local minimum at 12.09 kcal/mol higher in energy with respect to **51a** corresponding to an isomeric (hydrocyanide)(dihydroxy)copper(I) complex, **51b**. In complex **51b**, the Cu^+ ion is coordinated to HCN and two hydroxide ligands symmetrically arranged in a trigonal planar coordination geometry of Cu^+ without any HO···OH interaction (bop = −0.008), as is the case in **51a**. Complex **51a** is subsequently transformed to **28** or **35** via **52TS** with an activation barrier of 49.38 kcal/mol. The transformation of **51a** to **28** corresponds to an exothermic

process ($\Delta_R H = -11.81$ kcal/mol), while transformation to **35** is slightly endothermic ($\Delta_R H = 2.84$ kcal/mol). On the other hand, **51b** is transformed to **53**, being also a local minimum in the PES, through the same transition state **52TS**, with a lower activation barrier of 37.74 kcal/mol. In complex **53**, the Cu^+ ion is coordinated to an OH group and the remaining HCNOH moiety via an η^2-C,N bonding mode. The intermediate **53** evolves to yield **31**, through the transition state **54TS**, with an activation barrier of 19.48 kcal/mol. The transformation of **53** to **31** is predicted to be an exothermic reaction ($\Delta_R H = -50.12$ kcal/mol). It is obvious that Cu^+ ions have no catalytic effect on the oxidation of HCN to hydroxyformaldoxime by H_2O_2, but their role is restricted to the stabilization of the intermediates and products formed.

Dehydration Reactions of Hydroxyformaldoxime Conformers Catalyzed by Cu^+ Ions. A thorough inspection of the structures of the $Cu(hfaox)^+$ complexes given in Figures 4−6 illustrates that in some of them, namely, complexes **28**, **29**, **30**, **35**, **36**, and **41**, there exist favorable intramolecular interactions leading to elimination and concomitant coordination of a water molecule to the Cu^+ ion affording the $Cu(CHNO)(OH_2)^+$ complexes. Upon the basis of the geometry of the $Cu(hfaox)^+$ complexes, one would expect the most possible complexes formed to be $Cu(HCNO)(OH_2)^+$, **58**, and Cu(formylnitrene)-$(OH_2)^+$, **59**. The energy profiles of the reactions are depicted schematically in Figure 9, while the most significant geometrical parameters of all of the stationary points located at the B3LYP/6-311G(d,p) level on the PES governing the dehydration reaction are summarized in Figure 10. The coordination of the water molecule to $Cu(HCNO)^+$ and $Cu(formylnitrene)^+$ complexes to form **58** and **59**, respectively, is an exothermic process, the heat of reaction being 53.92 and 54.30 kcal/mol, respectively. The computed interaction energy of the water molecule with $Cu(HCNO)^+$ and $Cu(formylnitrene)^+$ complexes, being 53.26 and 54.97 kcal/mol, respectively, suggests the formation of a relatively weak $Cu-OH_2$ bond, which is also reflected in the small value of the bond overlap population (0.08). Moreover, the charge transferred from the water molecule to the Cu^+ ion amounts to 0.11 and 0.05 for complexes **58** and **59**, respectively.

The transformation of **37** to **58** (Figure 9a) proceeds via a reactant-like transition state, **55TS**, with a negligible activation barrier of only 4.31 kcal/mol and corresponds to an exothermic process ($\Delta_R H = -27.21$ kcal/mol). The activation barrier for the reverse reaction was predicted to be 33.60 kcal/mol, which is about half the value of the noncatalyzed reaction (Figure 2). Notice that **37** is stabilized with respect to the isolated reactants **7** and Cu^+ by 45.35 kcal/mol. The dehydration of both **28** and **41** (Figure 9a) was predicted to be a one-step process proceeding through **56TS** and **57TS**, with activation barriers of 53.49 and 39.35 kcal/mol, respectively. Both reactions are endothermic, the computed heats of reactions being 44.56 and 23.17 kcal/mol, respectively. Most important is the catalytic effect of Cu^+ ions on the reverse reaction, the addition of the water nucleophile to fulminic acid. The computed activation barriers for the exothermic addition reactions yielding **28** and **41** are 8.78 and 16.16 kcal/mol, respectively, much lower than the uncatalyzed reaction (Figure 2). Both transition states **56TS** and **57TS** are product-like with respect to the water addition reactions. In **56TS**, the water molecule approaching the C atom of **24** is symmetrical with respect to the plane defined by the O(1), C(2), N(3), and O(4) atoms. The C−O bond is lengthened by 0.18 Å, and the N−O bond is shortened by 0.14 Å in **56TS** with respect to **28**. Moreover, 0.18 charge unit are transferred from the nitrogen mainly toward the electrophilic carbon atom. The
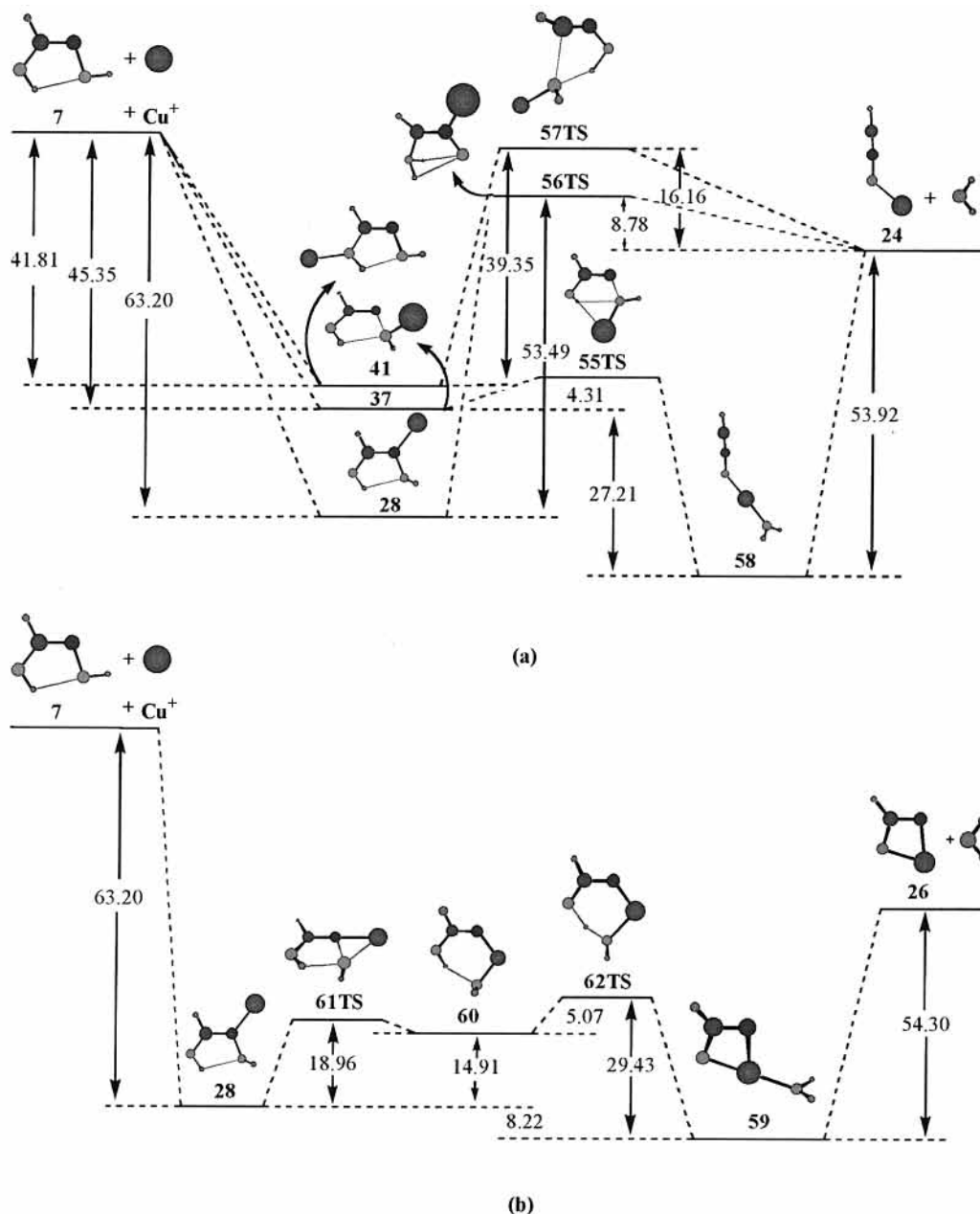
Figure 9. Energetic (kcal/mol) and geometric profile of the dehydration of hfaox to yield fulminic acid (a) or formylnitrene (b) in the presence of Cu^+ ions computed at the B3LYP/6-311G(d,p) level of theory.

imaginary frequency of **56TS** at 385i cm^{-1} corresponds to movements of the H atoms of the water molecule on the *xy* plane but in opposite directions. In **57TS**, the C−O bond is strongly lengthened by 0.88 Å and the N−O bond is shortened by 0.09 Å with respect to **41**. On the other hand, the C−N bond is shortened by 0.09 Å, while concomitantly the H atom of the HON− moiety is involved in the formation of a strong hydrogen bond with the O atom of the −COH moiety (bop = 0.10). Moreover, 0.17 charge unit is transferred via a cyclic pathway from the oxygen atom of the HON− moiety mainly toward the other oxygen atom, which acquires a higher negative net atomic charge by 0.27 charge unit with respect to **41**. Part of this electron density comes also from the coordinated Cu^+ ion, which loses 0.12 charge unit with respect to **41**. The imaginary frequency of **57TS** at 363i cm^{-1} corresponds to vibration mainly along the breaking C−O bond.

Finally, it was found that the alternative pathway of the dehydration of **28** to yield **59** proceeds in two steps (Figure

9b). The first step involves the insertion of the Cu^+ ion into the N−OH bond of **28** to afford the intermediate **60** through the transition state **61TS**, where the Cu^+ ion is coordinated to both the N and O atoms of the N−OH moiety. The computed activation barrier is 18.96 kcal/mol. The imaginary frequency of **61TS** at 146i cm^{-1} corresponds to movements of almost all atoms of the molecule. A transfer of 0.08 charge unit of electron density occurs from Cu to the coordinated O atom with a concomitant transfer of 0.08 charge unit from the N to the C atom in **61TS** with respect to **28**. The second step involves the transformation of the intermediate **60** to **59** via the transition state **62TS** with a relatively low activation barrier of 5.07 kcal/ mol. The imaginary frequency of **62TS** at 604i cm^{-1} corresponds to movements of the H atoms of the water molecule along the *x* coordinate leading to **59** or **60**. It should be noted that **62TS** exhibits a cyclic structure involving a strong hydrogen bond (bop values of the two O−H bonds being equal to 0.20 and 0.16, respectively). Considering now the reverse transfor-

Ab Initio Quantum Chemical Study

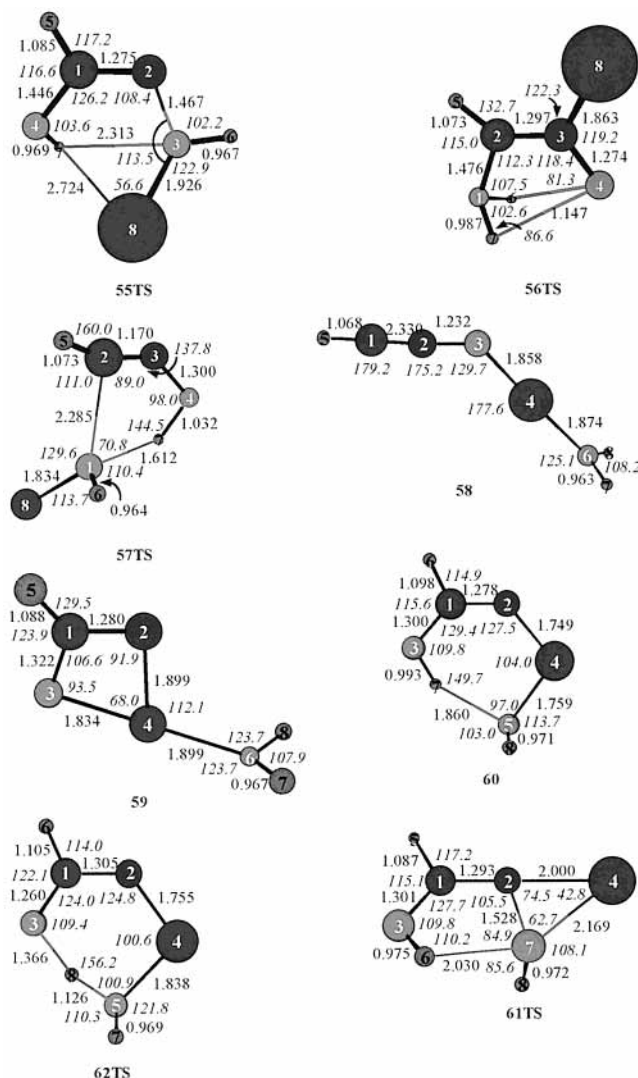*J. Phys. Chem. A, Vol. 106, No. 7, 2002* **1439**

Figure 10. Equilibrium structures (bond lengths in Å, bond angles in deg) of the stationary points located at the B3LYP/6-311G(d,p) level on the PES governing the dehydration of hfaox in the presence of Cu^+ ions.

mations **59 → 60** and **60 → 28**, it can be seen that the activation barriers are 29.43 and 4.03 kcal/mol, respectively, being much lower than that of the uncatalyzed reaction. In summary, there is no doubt that the Cu^+ ions catalyze the nucleophilic addition of water to nitrile oxides to form hydroxyformaldoxime conformers. Finally, it is worth noting that the water molecule in both complexes **58** and **59** is coordinated in a trans position with respect to the O donor atom of the coordinated fulminic and formylnitrene ligands (the $O-Cu-OH_2$ moiety is almost linear).

Conclusions

The use of first principles quantum chemical techniques at the HF, MP2, B3LYP, and CCSD(T) levels of theory using the 6-31G(d), 6-311G(d,p), 6-311+G(2df,2p), and 6-311++G(2d,p) basis sets in the exploration of the conformational space of hfaox yielded some interesting results. The most stable configuration among the eight possible isomers corresponds to the (*Z*)-(*s*-cis,*s*-trans) configuration, while the highest energy (*E*)-(*s*-trans,*s*-cis) conformer was found at 15.25, 15.31, 14.37, and 24.47 kcal/mol at the HF, MP2, B3LYP, and QCISD(T) levels of theory, respectively, using the largest 6-311++G(2d,p) basis set. From a methodological point of view, our results confirm the reliability

of the integrated computational tool formed by the B3LYP density functional model. This model has subsequently been used to investigate the dehydration products of hfaox and their associations with Cu^+ ions in an attempt to elucidate the role of Cu^+ ions in the hydration reactions of the CHNO isomers producing the hfaox conformers. Upon dehydration, hfaox could afford a number of isomeric CHNO species, the most stable being the isocyanic, cyanic, fulminic, and isofulminic acids, formylnitrene, and oxaziridinylidene. All dehydration processes are predicted to be endothermic. The reaction pathway for the addition of water to fulminic acid is predicted to occur via an activation barrier of 68.18 kcal/mol at the B3LYP/6-311G(d,p) level. The interaction of Cu^+ ions with the CHNO isomers and their precursor hfaox conformers for all possible bonding modes was also analyzed in the framework of DFT theory, illustrating that the Cu^+ ions show a preference for coordination with the N donor atoms. It was also found that Cu^+ ions have a strong catalytic effect on the dehydration reactions of hfaox to form CHNO isomers and are involved in a novel reaction of the oxidation of organic nitriles with hydrogen peroxide to yield oximes, stabilizing the reactants, products, and intermediates. The mechanisms of the respective reactions along with the structures and energetics of all copper(I) complexes, transition states, and intermediates are thoroughly discussed.

Supporting Information Available: Figures S1, S3, and S4 showing the Mulliken net atomic charges and bond overlap populations of hfaox conformers and their complexes with Cu^+ ions, Figures S2, S5, and S6 showing optimized geometries and relative stabilities of CHNO isomers and all possible species involved in the oxidation of organic nitriles with hydrogen peroxide to form oximes in the presence of Cu^+ ions, Tables S1 and S2 showing optimized structural parameters of hfaox conformers at selected levels of theory, Table S3 showing the relative energies, ΔE (kcal/mol), of the hfaox conformers at the selected levels of theory, Tables S4, S5, S7, and S9 showing the harmonic vibrational frequencies (cm^{-1}) and assignments of the bands of hfaox conformers, their dehydration CHNO isomeric products, and their complexes with Cu^+ ions, and Tables S6, S8, and S10 showing the GIAO/B3LYP/6-311+G(2df,2p)//B3LYP/6-311G(d,p) ^{13}C, ^{14}N, ^{17}O, and ^1H shielding tensor elements (σ, ppm). This material is available free of charge via the Internet at http://pubs.acs.org.

References and Notes

(1) Patai, S. In *The Chemistry of Cyanates and Their Thio Derivatives*; Feuer, H., Ed.; John Wiley & Sons: New York, 1977.

(2) Miller, J. A.; Bowman, C. T. *Prog. Energy Combust. Sci.* **1989**, *100*, 287.

(3) Perry, R. A.; Siebers, D. L. *Nature (London)* **1986**, *324*, 657.

(4) Poppinger, D.; Radom, L.; Pople, J. A. *J. Am. Chem. Soc.* **1977**, *99*, 7806.

(5) Teles, J. H.; Maier, G.; Hess, B. A., Jr.; Schaad, L. J.; Winnewisser, M.-B. P. *Chem. Ber.* **1989**, *122*, 753.

(6) Yokoyama, K.; Takane, S.-Y.; Fueno, T. *Bull. Chem. Soc. Jpn.* **1991**, *64*, 2230.

(7) East, A. L. L.; Johnson, C. S.; Allen, W. D. *J. Chem. Phys.* **1993**, *98*, 1299.

(8) Pinnavaia, N.; Bramley, M. J.; Su, M.-D.; Green, W. H.; Handy, N. C. *Mol. Phys.* **1993**, *78*, 319.

(9) Mebel, A. M.; Luna, A.; Lin, M. C.; Morokuma, K. *J. Chem. Phys.* **1996**, *105*, 6439.

(10) (a) Shaplay, W. A.; Bacskay, G. B. *J. Phys. Chem. A* **1999**, *103*, 4514. (b) Shaplay, W. A.; Bacskay, G. B. *J. Phys. Chem. A* **1999**, *103*, 6624.

(11) Poppinger, D.; Radom, L. *J. Am. Chem. Soc.* **1978**, *100*, 3674.

(12) Nguyen, M.-T.; Sana, M.; Leroy, G.; Dignam, K. G.; Hegarty, A. F. *J. Am. Chem. Soc.* **1980**, *102*, 573.

(13) Nguyen, M.-T.; Malone, S.; Hegarty, A. F.; Williams, I. I. *J. Org. Chem.* **1991**, *56*, 3683.

(14) Herhe, W. J.; Radom, L.; Schleyer, P. v. R.; Pople, J. A. *Ab initio Molecular Orbital Theory*; John Wiley & Sons: New York, 1986.

(15) Parr, R. G.; Yang, W. *Density Functional Theory of Atoms and Molecules*; Oxford University Press: New York, 1989.

(16) Frisch, M. J.; Trucks, G. W.; Schlegel, H. B.; Scuseria, G. E.; Robb, M. A.; Cheeseman, J. R.; Zakrzewski, V. G.; Montgomery, J. A., Jr.; Stratmann, R. E.; Burant, J. C.; Dapprich, S.; Millam, J. M.; Daniels, A. D.; Kudin, K. N.; Strain, M. C.; Farkas, O.; Tomasi, J.; Barone, V.; Cossi, M.; Cammi, R.; Mennucci, B.; Pomelli, C.; Adamo, C.; Clifford, S.; Ochterski, J.; Petersson, G. A.; Ayala, P. Y.; Cui, Q.; Morokuma, K.; Malick, D. K.; Rabuck, A. D.; Raghavachari, K.; Foresman, J. B.; Cioslowski, J.; Ortiz, J. V.; Stefanov, B. B.; Liu, G.; Liashenko, A.; Piskorz, P.; Komaromi, I.; Gomperts, R.; Martin, R. L.; Fox, D. J.; Keith, T.; Al-Laham, M. A.; Peng, C. Y.; Nanayakkara, A.; Gonzalez, C.; Challacombe, M.; Gill, P. M. W.; Johnson, B. G.; Chen, W.; Wong, M. W.; Andres, J. L.; Head-Gordon, M.; Replogle, E. S.; Pople, J. A. *Gaussian 98*, revision A.7; Gaussian, Inc.: Pittsburgh, PA, 1998.

(17) Schlegel, H. B. *J. Comput. Chem.* **1982**, *3*, 214.

(18) Conzalez, C.; Schlegel, H. B. *J. Phys. Chem.* **1989**, *90*, 2154.

(19) (a) Ditchfield, R. *Mol. Phys,* **1974**, *27*, 789. (b) Gauss, J. *J. Chem. Phys.* **1993**, *99*, 3629.

(20) (a) Pasinszki, T.; Westwood, N. P. C. *J. Phys. Chem.* **1995**, *99*, 6401. (b) Pasinszki, T.; Westwood, N. P. C. *J. Chem. Soc., Faraday Trans.* **1997**, *93*, 43. (c) Pasinszki, T.; Westwood, N. P. C. *J. Phys. Chem. A,* **1998**, *102*, 4939.

(21) Geiseler, G.; Böhling, H.; Fruwert, J. *J. Mol. Struct.* **1973**, *18*, 43.

(22) Harris, W. C.; Bush, S. F. *J. Chem. Phys.* **1972**, *56*, 6147.

(23) Scott, A. P.; Radom, L. *J. Phys. Chem.* **1996**, *100*, 16502.

(24) (a) Jameson, A. K.; Jameson, C. J. *Chem. Phys. Lett.* **1987**, *134*, 461 and references therein. (b) Hawkes, G. E.; Herwing, K.; Roberts, J. D. *J. Org. Chem.* **1974**, *39*, 1017.

(25) Olah, G. A.; Burrichter, A.; Rasul, G.; Hachoumy, M.; Surya Prakash, G. K. *Leibigs Ann. Chem.* **1988**, 1091.

(26) Tsoungas, P.; De Costa, B. F. *Org. Magn. Reson.* **1988**, *26*, 8.

(27) Wimmer, Z.; Saman, D.; Smoliková, J.; Romanuk, M. *J. Am. Chem. Soc.* **1997**, *119*, 12929.

(28) Jameson, C. J.; Jameson, A. K.; Oppussunggu, D.; Wile, S.; Burrel, P M.; Mason, J. *J. Chem. Phys.* **1981**, *74*, 81.

(29) Gainer, J.; Howarth, G. A.; Hoyle, W.; Roberts, S. *Org. Magn. Reson.* **1976**, *8*, 226.

(30) Yamada, K. *J. Mol. Spectrosc.* **1980**, *79*, 323.

(31) Mavridis, A.; Harrison, J. F. *J. Am. Chem. Soc.* **1980**, *102*, 7651.

(32) Koput, J.; Winnewisser, M.-B. P. *Chem. Phys Lett.* **1996**, *255*, 357.

(33) Rendell, A. P.; Lee, T. J.; Lindh, L. *Chem. Phys Lett.* **1992**, *194*, 84.

(34) Farnell, L.; Nobes, R. H.; Radom, L. *J. Mol. Spectrosc.* **1982**, *93*, 271.

(35) Maier, G.; Bothur, A.; Eckwert, J.; Reisenauer, H. P.; Stumpf, T. *Liebigs Ann./Recueil.* **1997**, 2505.

(36) Maier, G.; Teles, J. H.; Hess, B. A., Jr.; Schaad, L. J. *Angew. Chem., Int. Ed. Engl.* **1988**, *100*, 1014.

(37) Winnewisser, B. P.; Winnewisser, M.; Winther, F. *J. Mol. Spectrosc.* **1974**, *51*, 65.

(38) Bondybay, V. E.; English, J. H.; Mathews, C. W.; Cantolini, R. J. *J. Mol. Spectrosc.* **1982**, *92*, 431.

(39) Califano, S.; Lüttke, W. *Z. Phys. Chem.* **1956**, *6*, 83.

(40) Giguère, A.; Liu, I. D. *Can. J. Chem.* **1952**, *30*, 948.

(41) Cybulski, S. M.; Bishop, D. M. *J. Chem. Phys.* **1993**, *98*, 8057.

(42) Pople, J. A. *Proc. R. Soc. London, Ser. A* **1957**, *239*, 541.

(43) Beeler, A. J.; Orendt, A.; Mgrant, D. M.; Cutts, J.; Michl, P. W.; Zilm, K. W.; Downing, J. W.; Facelli, J. C.; Schnindler, M.; Kutzelnigg, W. *J. Am. Chem. Soc.* **1984**, *106*, 7672.

(44) Mason, J. In *Nuclear Magnetic Shielding and Molecular Structure*, Tossel, J. A., Ed.; Kluwer: Dordrecht, Netherlands, 1993; p 449.

(45) Duncan, T. M. *A Compilation of Chemical Shift Anisotropies*; Farragut: Chicago, 1990.

(46) Dahn, H.; Toan, V. V.; Pechy, P. *Magn. Reson. Spectrosc.* **1995**, *33*, 686.

(47) Boykin, D. W., Ed. ^{17}O *NMR Spectroscopy in Organic Chemistry*; CRC Press: Boca Raton, FL, 1990.

(48) Wasylishen, R. E.; Mooibroek, S.; Macdonald, J. B. *J. Chem. Phys.* **1984**, *81*, 1057.

(49) Dignam, K. J.; Hegarty, A. F.; Quain, P. L. *J. Chem. Soc., Perkin Trans.* **1977**, *2*, 1457; *J. Org. Chem.* **1978**, *43*, 388.

(50) Luna, A.; Amekraz, B.; Tortajada, J.; Morizur, J. P.; Mó, O.; Yánez, M. *J. Phys. Chem. A* **2000**, *104*, 3132.

(51) (a) Luna, A.; Morizur, J. P.; Tortajada, J.; Alcami, M.; Mó, O.; Yánez, M. *J. Phys. Chem. A* **1998**, *102*, 4652. (b) Luna, A.; Amekraz, B.; Morizur, J. P.; Tortajada, J.; Mó, O.; Yánez, M. *J. Phys. Chem. A* **1997**, *101*, 5931. (c) Alcami, M.; Mó, O.; Yánez, M.; Luna, A.; Morizur, J. P.; Tortajada, J. *J. Phys. Chem. A* **1998**, *102*, 10120.